2.12. Human hepatocellular carcinoma tissues

Twenty pairs of HCCs and adjacent nontumor counterparts were obtained at the time of surgical resection. All adjacent nontumor tissues were diagnosed as chronic hepatitis ($n=9$) or cirrhosis ($n=11$). Samples of normal liver tissue adjacent to hepatic metastatic tumors were obtained at the time of surgery and served as controls.

2.13. Statistical analysis

The data were analyzed with Statview software (SAS Institute Inc., Cary, NC) and are expressed as means ± standard deviation. The differences were compared using Bonferroni's *t*-test among group if one-way ANOVA showed $P<0.01$. The difference was considered statistically significant if $P<0.01$.

3. Results

3.1. Overexpression of ninjurin1 in human hepatoma cells

We introduced the ninjurin1 gene into Huh-7 cells as described in the Section 2 and established stable transfectants that constitutively expressed human ninjurin1. Among the four clones isolated, two, designated as Nin1 and Nin2, expressed relatively large amounts of human ninjurin1, judging from Western blot analyses. Nin1 and Nin2 showed approximately 2.3- and 2.5-fold increases in ninjurin1 protein, respectively, when compared to the mock clones, which had been transduced with an empty plasmid (Fig. 1(a)). In the immunocytochemical experiments, ninjurin1-transduced cells showed stronger expression of ninjurin1 than the mock clones (Fig. 1(c)). Of note is the finding that ninjurin1 overexpression caused dramatic alterations in cell morphology, as shown in Fig. 2. Nin1 and Nin2 cells exhibited increased size and a flattened morphology. No morphological change was observed in the mock clones.

Analysis of cell number after trypan blue staining revealed strong inhibition of cell growth in ninjurin1-overexpressing clones (Fig. 3). The parental and mock clones were maintained with a doubling time of approximately 36 h, whereas Nin1 and Nin2 had a doubling time of approximately 4 days.

3.2. Ninjurin1 provokes cell arrest

To determine the mechanisms of the reduced rate of cell growth, cell cycle analysis was conducted using flow cytometry. As shown in Fig. 4, ninjurin1 overexpression increased the percentage of the total cell population in the G0–G1 phase, decreased the percentage of cells in the S phase, but had no consistent effect on the percentage of cells in the G2-M phase, compared to the controls. Thus, ninjurin1-overexpressing cells were arrested at the G1 phase. We performed a TUNEL assay to examine the possible effects of enforced ninjurin1 expression on apoptosis. As shown in Fig. 5, the percentage of apoptotic cells in the ninjurin1-overexpressing clones was significantly lower than that in the control cells. Taken together,

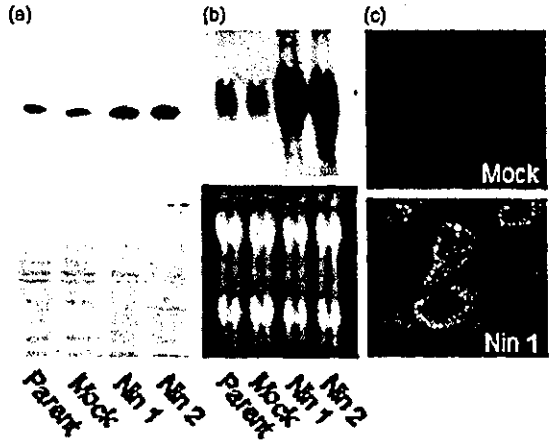

Fig. 1. Expression of ninjurin1 in ninjurin1-transfected Huh-7 cells. (a) (Top) Western blot analysis of ninjurin1 expression in control cells and ninjurin1-overexpressing clones (Nin1 and Nin2). (Bottom) The proteins visualized by Coomassie blue staining indicate that equal amounts of protein were loaded in each lane. One representative experiment of three is shown. (b) (Top) Northern blot analysis of ninjurin1 mRNA in the control cells and ninjurin1-overexpressing clones. (Bottom) Expressions of 18S and 28S rRNA indicate that equal amounts of RNA were loaded in each lane. (c) Immunocytochemical analysis of ninjurin1 expression in mock and Nin1 cells. Images were acquired at ×200 magnification by confocal laser microscopy using a Zeiss LSM510.

the growth-inhibitory effect of ninjurin1 was primarily due to cell cycle arrest rather than cell death.

3.3. Cell-cycle regulatory genes

To further characterize the nature of the cell-cycle arrest caused by ninjurin1 overexpression, the expression of several cell-cycle regulatory genes was examined by Western blot analysis. As shown in Fig. 6, the level of

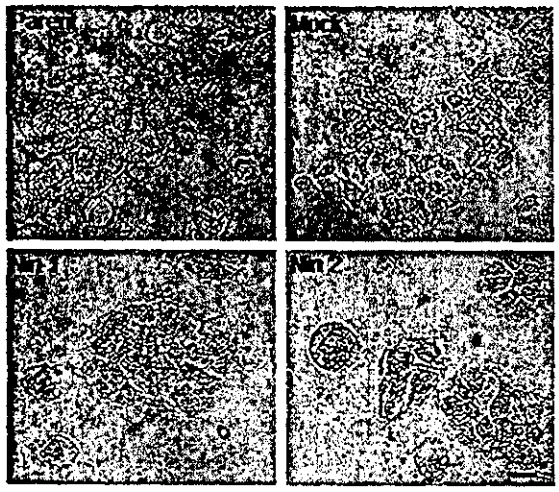

Fig. 2. Effect of ninjurin1 overexpression on cell morphology in Huh-7 cells. Phase contrast micrographs at ×200 magnification show the parental, mock-transfected, and ninjurin1-overexpressing Huh-7 cells (Nin1 and Nin2). Nin1 and Nin2 cells exhibited increased size and a flattened morphology. No changes in morphology were detected in the mock clones. (Bar = 50 μm).

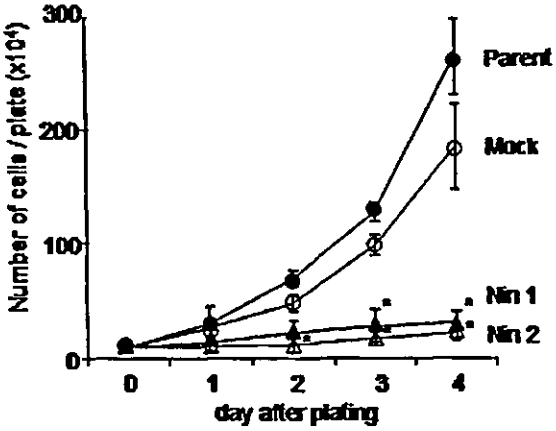

Fig. 3. Effect of ninjurin1 overexpression on cell growth. The total cell number was determined by trypan blue staining via microscopy at the times indicated. Data represent means±SD of three experiments performed in triplicate. (*$P<0.01$).

expression of cyclinA declined, but those of cyclinD and cyclinE were not altered in ninjurin1-overexpressing clones, when compared to the control clones. We next examined the expression of the catalytic partners of these cyclins, CDK2, CDK4, and CDK6. The levels of expression of all CDKs were consistently suppressed by ninjurin1 overexpression.

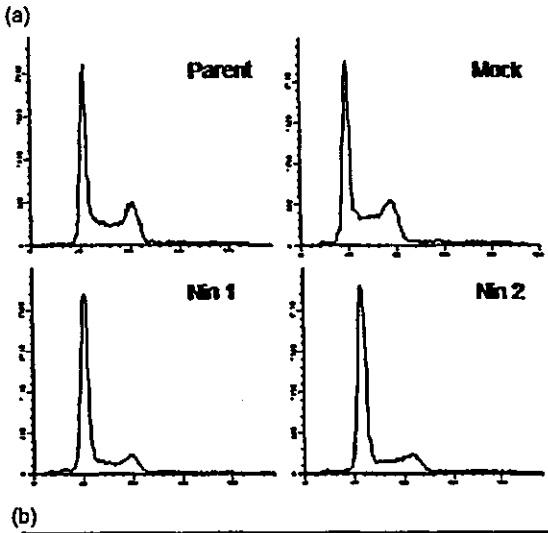

(b)

	Parent	Mock	Nin 1	Nin 2
G0/G1(%)	42±6.5	45±3.9	71±3.9*	66±4.7*
S (%)	44±6.0	38±4.8	22±4.5*	23±4.5*
G2/M(%)	14±1.5	17±2.5	7±0.8*	11±5.7

Fig. 4. Cell cycle profile of ninjurin1-overexpressing Huh-7 cells. (a) Cell cycle distribution of ninjurin1-overexpressing clones was analyzed by flow cytometry. Exponentially growing cultures of Huh-7 cells or their derivatives were trypsinized and collected. Propidium iodide-stained cells were analyzed by flow cytometry as described in Materials and Methods. (b) Values in the table indicate the percentage of the total cell population at the indicated phase of the cell cycle; data represent the means±SD of three experiments performed in triplicate. *$P<0.01$.

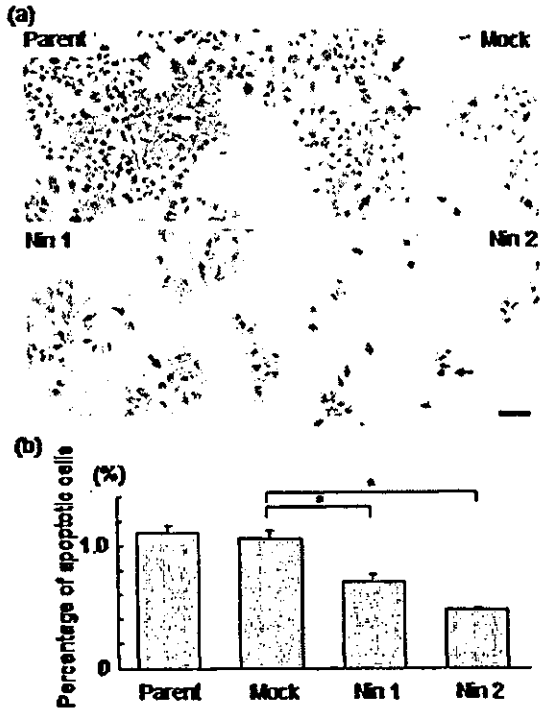

Fig. 5. Apoptotic effect of ninjurin1 overexpression in Huh-7 cells. (a) Apoptotic cells were detected by TUNEL assay. Apoptotic cells are indicated with arrows (Bar=20 μm). (b) Apoptotic cells with nuclei stained brown were counted under a light microscope, and their percentages are shown. *$P<0.01$.

We also examined the levels of expression of CDK inhibitors p21 and p27. There was no change in the level of p27, but the level of expression of p21 was greatly upregulated. On average, the expression level of p21 increased approximately 5-fold in both Nin1 and Nin2, compared to the mock clones. Northern blot analysis revealed that there was no apparent difference between the levels of p21 mRNA, whereas the mRNA levels of CDK2, CDK4, and CDK6 were repressed (Fig. 7(c)). These results indicated that CDK2, CDK4, and CDK6 expressions in Nin1 and Nin2 were transcriptionally downregulated, but p21 expression was not. In summary, enforced ninjurin1 expression resulted in elevated p21 and in repressed cyclinA, CDK2, CDK4, and CDK6 expression. The decline in the level of cyclinA expression is likely to be a consequence of the G1 arrest rather than its cause, since the products of this gene are believed to be one of the downstream events stimulated by E2F and to participate in the second half of the cell cycle [4].

The activity of the cyclin–CDK kinase complexes is tightly controlled by several mechanisms, including synthesis of the cyclin and CDK proteins, phosphorylation of CDK, and binding of CDK-inhibitory proteins [5]. We further examined CDK-associated kinase activity in the control cells and ninjurin1-overexpressing cells. As shown in Fig. 7(a), Rb phosphorylation by CDK2 immunoprecipitates, but not by CDK4 or CDK6 immunoprecipitates, was significantly decreased in the ninjurin1-overexpressing clones.

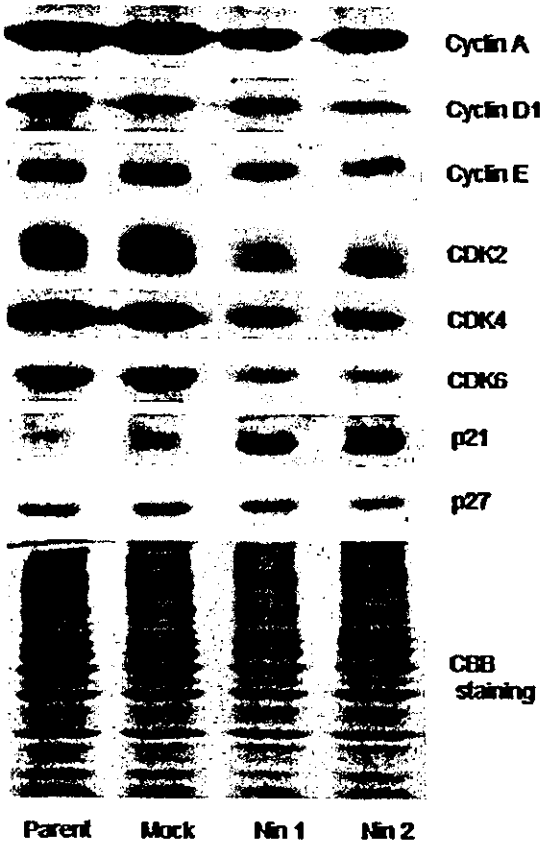

Fig. 6. Effect of ninjurin1 overexpression on cell cycle regulators in Huh-7 cells. Whole cell lysates (20 μg) extracted from the control cells and the ninjurin1-overexpressing clones were subjected to Western blot analysis with antibodies against cell-cycle regulators. The proteins visualized by Coomassie blue staining indicate that equal amounts of protein were loaded in each lane. One representative experiment of three is shown.

In addition, declines in the levels of hyperphosphorylated Rb (Fig. 7(b)) were also observed in ninjurin1-overexpressing clones. The data indicate that CDK2 activity, but not CDK4 or CDK6 activity, is downregulated in ninjurin1-overexpressing cells, although the levels of expression of all CDKs are consistently suppressed. Therefore, the levels of expression of CDKs do not seem to be important determinants for the CDK activities. It is more likely that inhibition of CDK2 activity is a consequence of ninjurin1-induced upregulation of p21, since p21 can efficiently inhibit cyclinE-CDK2 activity, but not cyclinD-dependent CDK4/6 activity [6]. Taken together, cell cycle arrest by enforced ninjurin1 expression seems to be associated with posttranscriptional elevation of p21 and a significant decrease in the CDK2 activity, but not CDK4 and CDK6 activities.

3.4. Cellular senescence

The observed characteristics, such as a flat enlarged morphology, arrest with a G1 DNA content, increased expression of p21 and resistance to spontaneous apoptosis, are similar to those of cells that have suppressed their

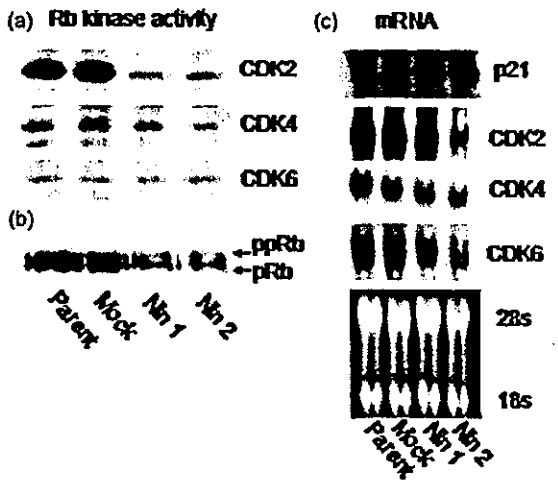

Fig. 7. Effect of ninjurin1 overexpression on CDKs and p21 in Huh-7 cells. (a) Analysis of CDK-associated Rb kinase activity in Huh-7 cells. CDKs were immunoprecipitated from whole cell lysates extracted from the control cells and the ninjurin1-overexpressing clones. The kinase activity of the immune complexes were measured using Rb protein as substrate. (b) Western blot analysis of the Rb protein in the control cells and the ninjurin1-overexpressing clones. ppRb indicates the hyperphosphorylated form of pRb. (c) Northern blot analysis of the CDKs and p21 mRNA in the control cells and the ninjurin1-overexpressing clones. Expression of 18S and 28S rRNA indicate that equal amounts of RNA were loaded in each lane.

proliferative capacity and become senescent [7–9]. Therefore, to investigate whether ninjurin1 induces cellular senescence, we examined two additional senescence-associated markers: detection of SA-β-galactosidase activity at pH 6.0 [10] and autofluorescence intensity [10,11]. Fig. 8 shows representative results of the SA-β-galactosidase activity. The percentage of SA-β-galactosidase-positive cells in ninjurin1-overexpressing populations was 26% in Nin1 and 21% in Nin2. In contrast, less than 1% of the parental and mock clones were SA-β-galactosidase-positive. The lysosomes of senescent cells accumulate lipofuscin, an autofluorescent pigment that is thought to be a heterogeneous mixture of lipid and protein products of peroxidation [11]. To determine the presence of autofluorescent pigments, we performed fluorescence microscopy on the Huh7 cells. As shown in Fig. 9(a), Nin1 and Nin2 cells displayed intense cytoplasmic, granular fluorescence. Flow cytometric analysis revealed that both Nin1 and Nin2 cells showed a discernable increase in fluorescence in comparison to the mock clones (Fig. 9(b)). Taken together, the data indicated that enforced expression of ninjurin1 induces not only cell-cycle arrest, but, more importantly, cellular senescence in hepatoma cells.

3.5. Expression of ninjurin1 in human liver tissues

We examined the expression of ninjurin1 by Western blot analysis in human liver tissues (Fig. 10). The levels of ninjurin1 expression in chronic diseased livers adjacent to HCC tissues increased in comparison with normal liver

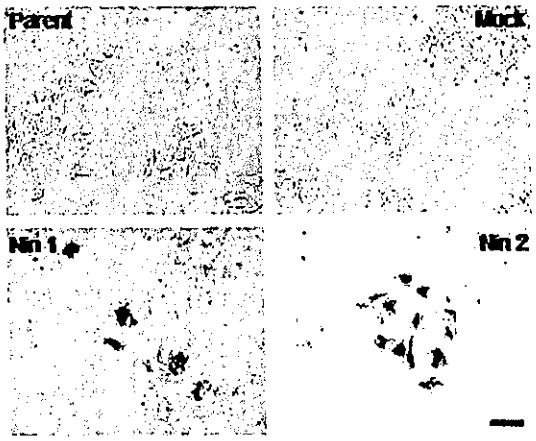

Fig. 8. Microscopic analysis of senescence-associated β-galactosidase staining in ninjurin1-overexpressing Huh-7 cells. Control cells and the ninjurin1-overexpressing clones cultured in 6-well plates were fixed and stained with senescence-associated β-gal staining kit as described in "Materials and Methods." Photomicrographs (×200) were obtained using a phase-contrast microscope (ECLIPSE TS 100, Nikon, Tokyo, Japan) (Bar = 50 μm).

tissues. Furthermore, the levels of ninjurin1 expression in HCC were significantly higher than those in the adjacent nontumor liver tissues. In other words, ninjurin1 expression was upregulated in chronic hepatitis or cirrhosis, and further increased in HCC. A recent report has shown that cellular senescence cells increase in the same order: normal liver, chronic hepatitis, and HCC [12]. This suggests that ninjurin1 is a mediator for activating the senescence program during the course of chronic liver disease.

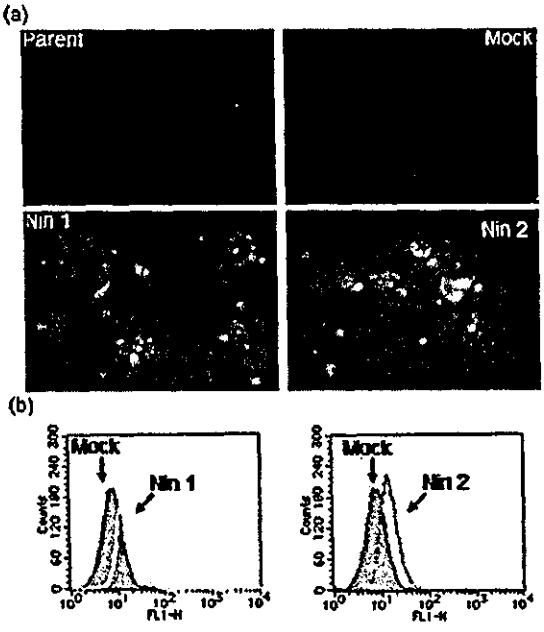

Fig. 9. Effect of ninjurin1 overexpression on autofluorescence in Huh-7 cells. (a) Fluorescent photomicrographs (×200) of the control cells and the ninjurin 1-overexpressing clones. (b) Flow cytometric analysis of ninjurin1-overexpressing Huh-7 cells on autofluorescence. The assay was performed in triplicate and the results are representative of three independent experiments.

4. Discussion

The present study clearly demonstrated that enforced expression of ninjurin1 upregulates p21 expression and triggers a cellular response leading to growth arrest and senescence in human hepatoma cells. Furthermore, increase of ninjurin1 expression was associated in vivo with both the development of HCC and the growth-inhibitory phase of liver regeneration (Fig. 10 and unpublished data). Ninjurin1-overexpressing clones displayed the following characteristics: (1) a flattened, enlarged cell morphology, G1 cell cycle arrest, and resistance to spontaneous apoptosis, which are commonly observed with senescent fibroblasts [13–15]; (2) accumulation of lipofuscin granules, which is a specific marker for senescent cells, evidenced by increased autofluorescence [11]; and (3) SA-β-galactosidase staining (pH 6.0), which is another specific biochemical marker of senescence [10]. Thus far, it has been established that ninjurin1 induces cell–cell adhesion by homophilic binding. The present study provides the first evidence that ninjurin1 provokes the cellular senescence program.

Human fibroblasts undergo a limited number of cell divisions before entering the irreversible arrest of senescence [16]. With regard to the molecular mechanisms in the senescence process, various kinds of genes, for example, p53 [17], Rb [18], and cell cycle regulator genes p21 [13,14] and p16 [15], are involved in establishing and maintaining

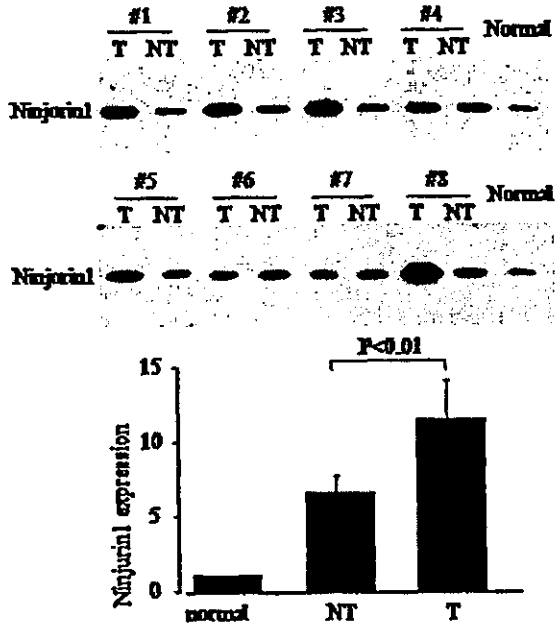

Fig. 10. Expression of ninjurin1 in human and animal liver. (a) Expression of ninjurin1 was assessed by Western blot analysis in 20 pairs of HCC (T), adjacent nontumor liver counterparts (NT), all of which were chronic diseased livers (NT), and two normal livers (normal). Shown is a representative blot. The optical density of each band was analyzed from the Scion image. Ninjurin1 expression in adjacent nontumor liver tissues was higher than in normal liver tissues, and that in HCC was higher than in adjacent nontumor liver tissues.

cellular senescence. These molecules commonly suffer loss-of-function mutations in various human cancers, and are recognized as tumor suppressors. The Huh-7 hepatoma cells used in the present study carry a mutated form of the p53 gene at codon 220 [19]. This mutant p53 lacks a DNA binding motif and is unable to induce p21 expression [20,21]. Therefore, the observed increase in p21 expression of the ninjurin1-expressing clones is independent of p53. In addition, Northern blot analysis indicated that the large increase in p21 protein expression was not due to an increase in transcription, but to posttranscriptional regulation. This mechanism is consistent with a recent report suggesting that the posttranscriptional induction of p21 is important for the establishment of cellular senescence [22]. Although the underlying mechanism is not clear, ninjurin1 is capable of increasing the expression of p21. Since p21 was originally identified via the phenomenon of senescence [13] and is thought to be one of the key regulators of senescence [14], p21 expression induced by ninjurin1 may be an important mediator in activating the senescence program.

Cellular senescence is not only observed in cultured cells such as fibroblasts [16] and mammary epithelial cells [23], but also occurs in vivo. In fact, senescent cells accumulate in chronic hepatitis, probably due to repeated destruction and regeneration of hepatocytes, and further increase in HCC tissue [12,24]. We found that ninjurin1 expression was upregulated in chronic hepatitis and further increased in HCC tissues, suggesting a role of ninjurin1 in mediating cellular senescence in chronic diseased livers as well as HCC. Cellular senescence is considered to function as a powerful tumor suppressive mechanism, limiting the proliferative capacity of cells in vivo [7,8]. Therefore, growth past senescent barriers may be a pivotal event in the earliest stages of carcinogenesis [12,23]. If so, hepatoma cells must acquire multiple alterations by which they can overcome ninjurin1-mediated senescence to grow in vivo. To better understand the role of ninjurin1 in the liver, further study is needed to examine whether inhibition of ninjurin1 expression affects senescence in hepatocytes as well as hepatocarcinogenesis.

Acknowledgements

This work was supported by a grant-in-aid (No. 1670499) from the Ministry of Education, Science, Sports, and Culture of Japan.

References

[1] Araki T, Milbrandt J. Ninjurin, a novel adhesion molecule, is induced by nerve injury and promotes axonal growth. Neuron 1996;17: 353–361.

[2] Araki T, Zimonjic DB, Popescu NC, Milbrandt J. Mechanism of homophilic binding mediated by ninjurin, a novel widely expressed adhesion molecule. J Biol Chem 1997;272:21373–21380.

[3] Chadwick BP, Heath SK, Williamson J, Obermayr F, Patel L, Sheer D, et al. The human homologue of the ninjurin gene maps to the candidate region of hereditary sensory neuropathy type I (HSNI). Genomics 1998;47:58–63.

[4] Slansky JE, Farnham PJ. Introduction to the E2F family: protein structure and gene regulation. Curr Top Microbiol Immunol 1996; 208:1–30.

[5] Morgan DO. Principles of CDK regulation. Nature 1995;374: 131–134.

[6] Sherr CJ, Roberts JM. CDK inhibitors: positive and negative regulators of G1-phase progression. Genes Dev 1999;13:1501–1512.

[7] Campisi J. Cancer, aging and cellular senescence. In vivo 2000;14: 183–188.

[8] Wynford-Thomas D. Cellular senescence and cancer. J Pathol 1999; 187:100–111.

[9] Shiratori Y, Shiina S, Imamura M, Kato N, Kanai F, Okudaira T, et al. Characteristic difference of hepatocellular carcinoma between hepatitis B- and C-viral infection in Japan. Hepatology 1995;22:1027–1033.

[10] Goodwin EC, Yang E, Lee CJ, Lee HW, DiMaio D, Hwang ES. Rapid induction of senescence in human cervical carcinoma cells. Proc Natl Acad Sci USA 2000;97:10978–10983.

[11] von Zglinicki T, Nilsson E, Docke WD, Brunk UT. Lipofuscin accumulation and ageing of fibroblasts. Gerontology 1995;41:95–108.

[12] Paradis V, Youssef N, Dargere D, Ba N, Bonvoust F, Deschatertte J, et al. Replicative senescence in normal liver, chronic hepatitis C, and hepatocellular carcinomas. Human Pathol 2001;32:327–332.

[13] Noda A, Ning Y, Venable SF, Pereira-Smith OM, Smith JR. Cloning of senescent cell-derived inhibitors of DNA synthesis using an expression screen. Exp Cell Res 1994;211:90–98.

[14] Brown JP, Wei W, Sedivy JM. Bypass of senescence after disruption of $p21^{CIP1/WAF1}$ gene in normal diploid human fibroblasts. Science 1997;277:831–834.

[15] Hara E, Smith R, Prry D, Tahara H, Peeters G. Regulation of $p16^{CDKN2}$ expression and its implications for cell immortalization and senescence. Mol Cell Biol 1996;16:859–867.

[16] Hayflick L, Moorhead PS. The serial cultivation of human diploid cell strains. Exp Cell Res 1961;25:585–621.

[17] Sugrue MM, Shin DY, Lee SW, Aaronson SA. Wild-type p53 triggers a rapid senescence program in human tumor cells lacking functional p53. Proc Natl Acad Sci USA 1997;94:9648–9653.

[18] Shay JW, Pereira-Smith OM, Wright WR. A role for both RB and p53 in the regulation of human cellular senescence. Exp Cell Res 1991; 196:33–39.

[19] Hsu IC, Tokiwa T, Bennett W, Metcalf RA, Welch JA, Sun T, et al. p53 gene mutation and integrated hepatitis B viral DNA sequences in human liver cancer cell lines. Carcinogenesis 1993; 14:987–992.

[20] Jia LQ, Osada M, Ishioka C, Gamo M, Ikawa S, Suzuki T, et al. Screening the p53 status of human cell lines using a yeast functional assay. Mol Carcinog 1997;19:243–253.

[21] Campomenosi P, Monti P, Aprile A, Abbondandolo A, Frebourg T, Gold B, et al. p53 mutants can often transactivate promoters containing a p21 but not Bax or PIG3 responsive elements. Oncogene 2001;20:3573–3579.

[22] Burkhart BA, Alcorta DA, Chiao C, Isaacs JS, Barrett JC. Two posttranscriptional pathways that regulate p21 (Cip1/Waf1/Sdi1) are identified by HPV16-E6 interaction and correlate with life span and cellular senescence. Exp Cell Res 1999;247:168–175.

[23] Romanov SR, Kozakiewicz BK, Holst CR, Stampfer MR, Haupt LM, Tisty TD. Normal human mammary epithelial cells spontaneously escape senescence and acquire genomic changes. Nature 2001;409: 633–637.

[24] Wiemann SU, Satyanarayana A, Tsahuridu M, Tillmann HL, Zender L, Klempnauer J, et al. Hepatocyte telomere shortening and senescence are general markers of human liver cirrhosis. FASEB J 2002;16:935–942.

GASTROENTEROLOGY 2004;127:1189–1197

Hepatocyte-Specific Disruption of Bcl-x_L Leads to Continuous Hepatocyte Apoptosis and Liver Fibrotic Responses

TETSUO TAKEHARA,* TOMOHIDE TATSUMI,* TAKAHIRO SUZUKI,* EDMUND B. RUCKER III,† LOTHAR HENNIGHAUSEN,§ MASAHISA JINUSHI,* TAKUYA MIYAGI,* YOSHIYUKI KANAZAWA,* and NORIO HAYASHI*

*Department of Molecular Therapeutics, Osaka University Graduate School of Medicine, Osaka, Japan; †Animal Sciences Unit, University of Missouri, Columbia, Missouri; and §Laboratory of Genetics and Physiology, National Institute of Diabetes and Digestive and Kidney Diseases, National Institutes of Health, Bethesda, Maryland

Background & Aims: Recent research has suggested that apoptosis could be involved in the development of fibrosis, although it is generally considered to be a mechanism of cell removal without consequences to the tissue. Bcl-x_L, an antiapoptotic member of the Bcl-2 family, is expressed in hepatocytes and up-modulated during various pathologic conditions. The aim of this study was to explore the function of Bcl-x_L in hepatocytes using the Cre-*lox*P system and to analyze the consequences of long-term apoptosis in hepatocytes. *Methods:* Hepatocytes isolated from mice homozygous for a floxed *bcl-x* allele (*bcl-x fl/fl*) were infected with recombinant adenovirus expressing the Cre recombinase gene (AdexCre). *Bcl-x fl/fl* mice were crossed with *Alb*-Cre transgenic mice, which express Cre under regulation of the albumin gene promoter to generate hepatocyte-specific Bcl-x_L-deficient mice. *Results:* On AdexCre infection, primary cultured *bcl-x fl/fl* hepatocytes reduced their expression of Bcl-x_L and rapidly underwent apoptosis associated with mitochondrial damage. In vivo hepatocyte-specific disruption of Bcl-x_L resulted in spontaneous apoptosis of hepatocytes for more than 6 months. The Bcl-x_L-deficient mice showed liver fibrosis with advanced age that was preceded by an increase in hepatic transforming growth factor β production. In vitro, macrophages and hepatocytes produced transforming growth factor β on exposure to apoptotic hepatocytes. *Conclusions:* The present study identified Bcl-x_L as a critical apoptosis antagonist in hepatocytes. Furthermore, it offers proof that persistent apoptosis of parenchymal cells is sufficient to induce fibrotic responses and suggests a mechanistic link between apoptosis and fibrosis.

Apoptosis is generally considered to be a mechanism of cell removal without consequences to the tissues.[1] This presumption mainly comes from the observations during organogenesis, where apoptosis is used for programmed and orchestrated deletion of unwanted cells. Apoptosis is also frequently observed after birth in vital organs with various insults; apoptotic loss of parenchymal cells followed by collagen deposition is the key feature of chronic injury of organs, such as the liver[2,3] and lung.[4] Although this suggests a link between apoptosis and fibrosis, there has been no clear evidence supporting that apoptosis induces fibrosis in vivo.

We previously reported that Bcl-x_L, an antiapoptotic member of the Bcl-2 family, is overexpressed in a subset of human hepatocellular carcinomas and plays a critical role in the survival of hepatoma cells under stress-inducing conditions.[5] Bcl-x_L is also expressed in nontransformed hepatocytes and is up-modulated during the course of liver regeneration[6] as well as in some forms of liver injury,[7] which may be correlated with the survival advantage of hepatic cells. However, the functional relevance of this molecule in the adult liver has not been established, because targeted deletion of the *bcl-x* gene in the mouse leads to embryonic lethality due to abnormal neuronal development and a defect in hematopoiesis.[8]

Here we show that hepatocyte-specific Bcl-x_L-deficient mice develop spontaneous and continuous apoptosis in hepatocytes, identifying Bcl-x_L as a crucial apoptosis antagonist for this cell type. Of interest is the finding that the mice develop intralobular liver fibrosis with advanced age, providing in vivo evidence for a direct link between apoptosis and fibrosis. We also show that hepatocytes as well as macrophages can produce transforming growth factor (TGF)-β when engulfing apoptotic cells and raise the possibility that excessive and prolonged production of TGF-β may be a mechanism by which apoptosis of parenchymal cells induces fibrotic responses.

Abbreviations used in this paper: MOI, multiplicity of infection; TGF, transforming growth factor; TUNEL, terminal deoxynucleotidyl transferase–mediated deoxyuridine triphosphate nick-end labeling.

0016-5085/04/$30.00
doi:10.1053/j.gastro.2004.07.019

Materials and Methods

Mice

Mice carrying a *bcl-x* gene with 2 *lox*P sequences at the promoter region and the second intron (floxed *bcl-x* gene) have been described previously.[9] The background of the mice is a 129SvEv/C57BL6 mix. *Bcl-x fl/fl* mice and *bcl-x* +/+ mice were generated by heterozygous crosses and verified by tail DNA biopsies followed by polymerase chain reaction analysis. *Bcl-x fl/fl* mice were crossed with *Alb-Cre* transgenic mice,[10] which express the Cre recombinase gene under the control of the albumin gene promoter. *Alb (+)* (i.e., knockdown) and *Alb (−)* (i.e., littermate controls) *bcl-x fl/fl* mice for the experiments were generated by mating *Alb (+) bcl-x fl/fl* male mice with *bcl-x fl/fl* female mice. To establish severe liver fibrosis as a control, we injected Balb/cA mice with 6 μL of carbon tetrachloride dissolved in mineral oil 2 times a week for 6 weeks as previously reported.[11] All animals were housed under specific pathogen–free conditions and treated with humane care under approval from the Animal Care and Use Committee of Osaka University Medical School.

Adenovirus

Recombinant adenoviruses, AdexCre and AdexLacZ, which express the Cre recombinase gene and the β-galactosidase gene, respectively, under the control of the CAG promoter, were purchased from Takara Shuzo (Tokyo, Japan). A concentrated and purified virus stock was prepared, and titers of the purified viral stock were determined as described previously.[12]

Primary Culture of Hepatocytes

Livers were digested using a standard in situ 2-step collagenase perfusion procedure (Gibco BRL, Rockville, MD). Hepatocytes were isolated from nonparenchymal cells by subsequent centrifugation at 50*g* for 1 minute. In a selected experiment, nonparenchymal cells in the supernatant were pelleted at 400*g* for 5 minutes and applied for Western analysis. Isolated hepatocytes with >90% viability were cultured in Williams' medium E containing 10% fetal calf serum. Six hours after plating, hepatocytes were infected with AdexCre for 2 hours and further cultured after replacement with fresh medium.

Western Blot

Whole-cell extracts from cultured cells or tissues were prepared and subjected to Western blot analysis. Detection of Bcl-x_L was performed as shown previously.[5,13] Bcl-2, Mcl-1, Bcl-w, the cleaved form of caspase-3, and glyceraldehyde-3-phosphate dehydrogenase were detected by using anti–Bcl-2 antibody (Transduction Laboratories, Lexington, KY), anti–Mcl-1 antibody (Santa Cruz Biotechnology, Santa Cruz, CA), anti–Bcl-w antibody (R&D Systems, Minneapolis, MN), anti-cleaved caspase-3 antibody (Cell Signaling Technology, Beverly, MA), and anti–glyceraldehyde-3-phosphate dehydrogenase antibody (Trevigen, Gaithersburg, MD), respectively. Preparation of cytosolic fraction of cultured hepatocytes and detection of cytochrome *c* by Western blot was described previously.[13]

Cell Viability Assay

Hepatocytes isolated from *bcl-x fl/fl* mice or their *bcl-x* +/+ littermates were plated in a 96-well plate. Six hours later, the cells were treated with or without AdexCre at a multiplicity of infection (MOI) of 3 for 2 hours. Standard 3-(4,5-dimethylthiazol-2-yl)-2,5-diphenyltetrazolium bromide assay was performed every 24 hours. The percentage viability of cultured hepatocytes after AdexCre infection was calculated by using uninfected hepatocytes as a control at each time point. Cells were also stained with acridine orange and ethidium bromide for 10 minutes and fixed with paraformaldehyde to examine apoptotic nuclei.

Histology and Immunohistochemistry

The formalin-fixed livers were paraffin embedded, and liver sections were analyzed by H&E staining. Deparaffinized liver sections were stained with anti-Cre recombinase antibody (American Research Product, Belmont, MA) and anti-cleaved caspase-3 antibody (Cell Signaling Technology). Bound primary antibody was visualized by using the ABC system (Vector Laboratories, Burlingame, CA). Terminal deoxynucleotidyl transferase–mediated deoxyuridine triphosphate nick-end labeling (TUNEL) staining was performed by using an ApopTag kit according to the manufacturer's instructions (Serological Corporation, Norcross, GA).

Electron Microscopy

The livers were fixed via the inferior vena cava with a fixative containing 2% glutaraldehyde and 2% paraformaldehyde in 0.1 mol/L phosphate buffer for 5 minutes. The liver sections were then postfixed with OsO_4, dehydrated in gradient ethanol, and embedded. Ultrathin sections were viewed with a Hitachi 7000 electron microscope (Tokyo, Japan).

Hepatic Hydroxyproline

Anterior median lobes of the frozen liver samples were subjected to analysis of hydroxyproline content, as previously described.[11]

Hepatic TGF-β1 Analysis

Liver specimens were lysed with Tris-buffered saline with 1% Nonidet P-40 and 10% glycerol. After being activated by hydrogen chloride, the lysate was analyzed for TGF-β1 by using an enzyme-linked immunosorbent assay kit (R&D Systems).

Coculture Experiment

Bcl-x fl/fl hepatocytes were infected with AdexCre for 2 hours at an MOI of 3. After 48 hours, the floating apoptotic cells were collected from dishes by centrifugation, washed 3 times, and resuspended in Dulbecco's modified Eagle medium. A murine macrophage line, Raw264.7 (American Type Culture Collection, Rockville, MD), and

hepatocytes isolated from wild-type mice were incubated in 24-well plates at 37°C in Dulbecco's modified Eagle medium containing the apoptotic hepatocytes (a ratio of apoptotic cells to Raw264.7 or hepatocytes of 5:1). The incubation was also performed using Transwell membrane to separate apoptotic cells from Raw264.7 cells or hepatocytes. After 18 hours, the supernatant was acid activated and examined for the concentration of TGF-β1 by enzyme-linked immunosorbent assay. In selected experiments, apoptotic hepatocytes were labeled with 10 μmol/L of 5(6)-carboxytetramethylrhodamine–succinimidyl ester (Sigma Chemical Co., St. Louis, MO) and then rinsed with media. Engulfment of apoptotic hepatocytes was determined by fluorescence microscopy.

Statistics

Data are presented as mean ± SD. Comparisons between groups were performed by unpaired *t* test with Welch's correction or analysis of variance for experiments with more than 2 subgroups. Post hoc tests were performed using Bonferroni's *t* test. $P < 0.05$ was considered statistically significant.

Results

Bcl-x_L–Deficient Hepatocytes Undergo Spontaneous Apoptosis In Vitro and In Vivo

Among antiapoptotic members of the Bcl-2 family, hepatocytes expressed Bcl-x_L, Bcl-w, and Mcl-1 but not Bcl-2 (Figure 1*A*). To explore the function of Bcl-x_L in hepatocytes, we deleted the gene specifically in these cells using a Cre-*loxP*–based recombination. Mice had been generated that carried *lox*P sites in the promoter and the second intron of the *bcl-x* gene.[9] Primary hepatocytes were isolated from mice homozygous for the floxed *bcl-x* allele (*bcl-x fl/fl*) and infected with AdexCre, an adenoviral vector that expresses Cre recombinase. In AdexCre infection, the *bcl-x* gene was deleted (data not shown) and Bcl-x_L levels were greatly reduced (Figure 1*B*). The viability of the *bcl-x fl/fl* hepatocytes decreased 2 days after AdexCre infection, whereas hepatocytes isolated from *bcl-x* +/+ littermates survived (Figure 1*C*). Mitochondrial damage preceded the decrease in cellular viability, because cytochrome *c* was clearly detected in

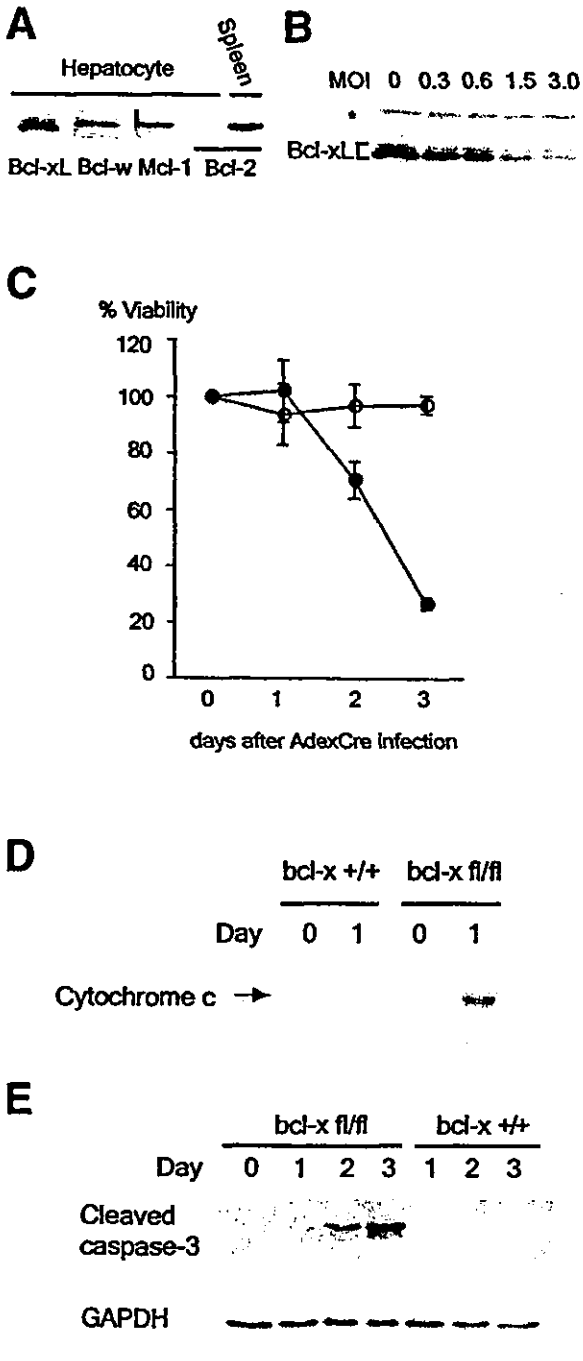

Figure 1. Bcl-x_L–deficient hepatocytes undergo spontaneous apoptosis in vitro. (*A*) Western blot analysis for the expression of antiapoptotic members of the Bcl-2 in primary cultured murine hepatocytes. Spleen is used as a positive control for Bcl-2 expression. (*B*) AdexCre infection down-regulates Bcl-x_L expression in primary cultured *bcl-x fl/fl* hepatocytes. Primary cultured *bcl-x fl/fl* hepatocytes were infected with AdexCre at the indicated MOI. Western blot analysis for Bcl-x_L at 36 hours after AdexCre infection is shown. Bcl-x_L migrates as a doublet band as shown previously.[13] *, nonspecific band. (*C*) 3-(4,5-dimethylthiazol-2-yl)-2,5-diphenyltetrazolium bromide viability assay of primary cultured *bcl-x fl/fl* (*closed circles*) or *bcl-x* +/+ (*open circles*) hepatocytes after AdexCre infection at an MOI of 3. (*D*) Detection of cytochrome *c* in the cytosolic fraction of cultured hepatocytes. The S-100 fraction was prepared from hepatocytes before and 1 day after AdexCre infection. Release of cytochrome *c* into the cytosol was examined by Western blot analysis. (*E*) Western blot analysis for the cleaved form of caspase-3 in *bcl-x fl/fl* and *bcl-x* +/+ hepatocytes at indicated time points after AdexCre infection (MOI of 3). To assess loading variability, membranes were reprobed with anti–glyceraldehyde-3-phosphate dehydrogenase antibody. All experiments were performed at least 3 times, and representative results are shown.

the S-100 fraction of *bcl-x fl/fl* hepatocytes at 24 hours after AdexCre infection (Figure 1*D*). The decreased viability observed in hepatocytes with reduced levels of Bcl-x_L was associated with increased apoptosis, as evidenced by caspase activation (Figure 1*E*) as well as typical nuclear changes (percentage of apoptotic nucleus-positive *bcl-x fl/fl* hepatocytes vs. *bcl-x* +/+ hepatocytes 2 days after AdexCre infection, 60% ± 19% vs. 7% ± 4%, respectively; $P < 0.05$). To examine the consequences of reduced Bcl-x_L levels in hepatocytes in vivo, we injected AdexCre into the tail vein, because intravenous injection of adenoviral vectors preferentially transduces hepatocytes.[14] More than 80% of the hepatocytes expressed Cre, and the levels of Bcl-x_L were substantially reduced in the *bcl-x fl/fl* livers 3 days after injection (Figure 2*A* and *B*). At this time point, TUNEL-positive hepatocytes were scattered in the lobules in the *bcl-x fl/fl* mice but rarely observed in their *bcl-x* +/+ littermates (13.5 ± 5.3 and 0.8 ± 0.6/field, respectively; $P < 0.05$) (Figure 2*C*). Moreover, the levels of serum alanine aminotransferase, an index of hepatocyte injury, were significantly higher in AdexCre-injected *bcl-x fl/fl* than *bcl-x* +/+ mice (760 ± 360 vs. 70 ± 13 IU/L; $P < 0.05$). These results indicate, for the first time, that Bcl-x_L plays an indispensable role in maintaining the integrity of hepatocytes in vivo as well as in vitro.

Hepatocyte-Specific Bcl-x_L–Deficient Mice: A Model of Long-term Spontaneous Apoptosis in the Liver

To disrupt Bcl-x_L constitutively as well as more specifically in hepatocytes, *bcl-x fl/fl* mice were crossed with *Alb-Cre* transgenic mice, which express the Cre recombinase gene under regulation of the albumin gene promoter.[10] Mice homozygous for the floxed *bcl-x* allele that carried the *Alb-Cre* transgene (*Alb* [+] *bcl-x fl/fl*) were born at the Mendelian frequency and developed normally. As expected, a reduction of Bcl-x_L in these mice occurred specifically in hepatocytes (Figure 3*A*). The constitutive knockdown of Bcl-x_L did not affect the levels of expression of other Bcl-2–related molecules, such as Mcl-1, Bcl-w, Bak, and Bax, in the liver (not shown). In agreement with the findings of the AdexCre-injected model, we observed an increase in apoptotic hepatocytes with typical morphologic characteristics scattered in the liver lobule of the *Alb* (+) *bcl-x fl/fl* mice, as compared with their *Alb* (−) *bcl-x fl/fl* littermates (Figure 3*B*). *Alb-Cre* transgenic mice carrying 2 wild-type *bcl-x* alleles did not display such liver pathology (data not shown). Apoptosis in *Alb* (+) *bcl-x fl/fl* livers

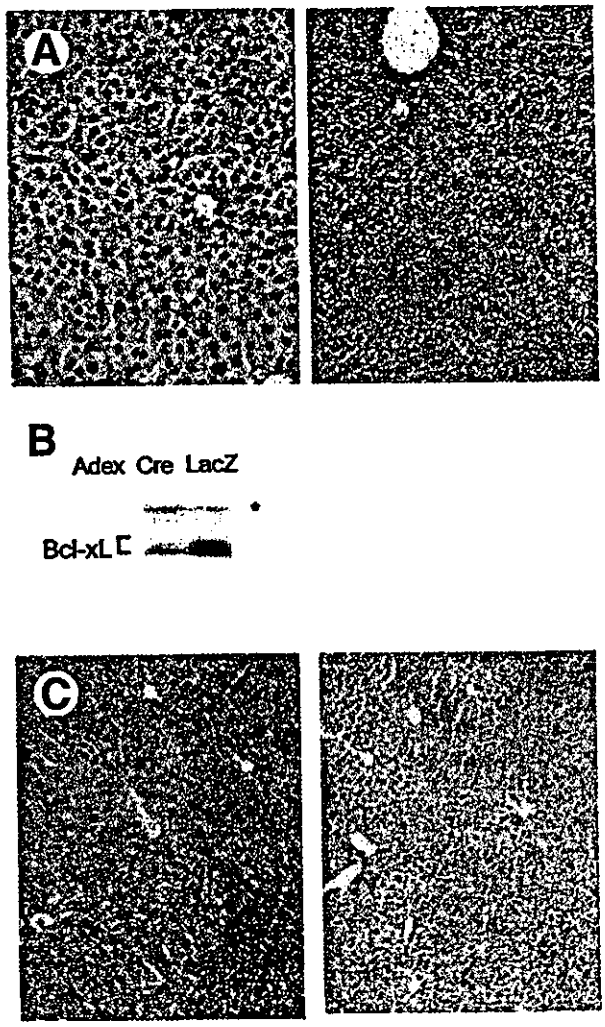

Figure 2. Bcl-x_L–deficient hepatocytes undergo apoptosis in vivo. (*A*) Immunohistochemical detection of Cre in the liver of *bcl-x fl/fl* mice 3 days after receiving 3×10^9 plaque-forming units of either AdexCre (*left*) or AdexLacZ (*right*). Note that >80% of the hepatocytes express Cre in the nuclei after AdexCre injection. (*B*) Western blot analysis of Bcl-x_L in the livers of *bcl-x fl/fl* mice 3 days after receiving 3×10^9 plaque-forming units of either AdexCre or AdexLacZ. *, nonspecific band. (*C*) TUNEL staining of the liver section of *bcl-x fl/fl* (*left*) or *bcl-x* +/+ (*right*) mice 3 days after AdexCre (3×10^9 plaque-forming units) injection. All experiments were performed at least 3 times, and representative figures are shown.

was confirmed by TUNEL staining as well as in situ cleaved caspase-3 staining (Figure 3*C*). Our electron microscopic studies revealed that the mitochondrial alterations, such as disruption of outer mitochondrial membrane and herniation of the matrix, appeared in apoptotic hepatocytes in *Alb* (+) *bcl-x fl/fl* mice (Figure 3*D*). Liver injury was observed in *Alb* (+) *bcl-x fl/fl* mice as early as 1 month after birth and persisted for at least 7 months, which was our period of observation (Figure 3*E* and *F*). These data confirm the critical role of Bcl-x_L in suppressing apoptosis in hepatocytes in the liver. Moreover, *Alb* (+) *bcl-x fl/fl* mice provide a unique

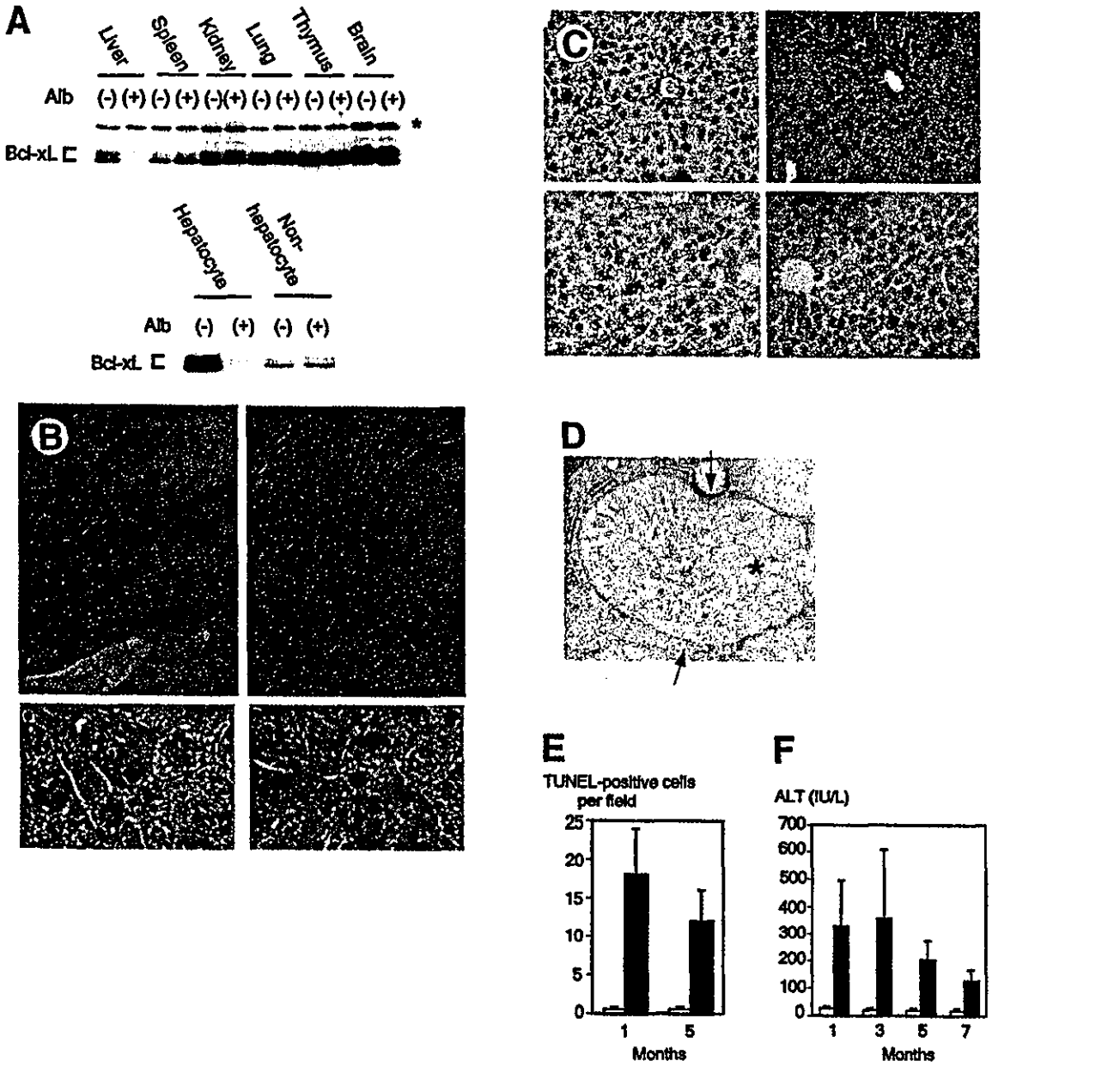

Figure 3. Constitutive knockdown of Bcl-x_L leads to spontaneous and continuous apoptosis in hepatocytes. (*A*) Hepatocyte-specific knockdown of Bcl-x_L. Various organs obtained from *Alb (+) bcl-x fl/fl* and *Alb (−) bcl-x fl/fl* mice were subjected to Western blot analysis of Bcl-x_L (*upper blot*). Hepatocytes as well as nonparenchymal cells in the livers were separated by in situ collagenase perfusion followed by centrifugation and were examined for Bcl-x_L expression (*lower blot*). *, nonspecific band. (*B*) H&E staining of the liver section. Hepatocyte apoptosis characterized by cellular shrinkage and condensed nuclei in the *Alb (+) bcl-x fl/fl* liver (*upper left*) increased in comparison with that in the liver of their *Alb (−) bcl-x fl/fl* littermates (*upper right*). Representative figures of apoptotic hepatocytes engulfed by neighboring hepatocytes (*lower left*) and nonparenchymal cells (*lower right*) in the *Alb (+) bcl-x fl/fl* liver section. *Arrows* indicate apoptotic hepatocytes, and *arrowheads* indicate engulfed apoptotic hepatocytes. (*C*) Immunohistochemical detection of the cleaved form of caspase-3 (*upper panels*) and TUNEL staining (*lower panels*) of the liver sections of *Alb (+) bcl-x fl/fl* (*left panels*) and *Alb (−) bcl-x fl/fl* mice (*right panels*). Representative figures are shown. Note that a small but significant number of hepatocytes were positive for the cleaved form of caspase-3 in the cytoplasm and were also positive for DNA breaks in the nuclei. (*D*) Electron micrograph showing mitochondrial damage in apoptotic hepatocytes of the *Alb (+) bcl-x fl/fl* liver. The outer membrane of the mitochondria was disrupted (*arrows*), while parts of the inner membrane appeared herniated through this gap (*). Whereas the cristae were tightly folded in that part of the mitochondrion in which the outer membrane appeared intact, the cristae were reduced or absent in the defective herniated part of the inner membrane. (Original magnification 30,000×.) (*E*) The number of TUNEL-positive cells and (*F*) serum alanine aminotransferase values of *Alb (+) bcl-x fl/fl* (■) and *Alb (−) bcl-x fl/fl* (□) mice at various months after birth.

opportunity to analyze the consequences of long-term apoptosis specifically occurring in hepatocytes.

Mice Lacking Hepatic Bcl-x_L Expression Develop Intralobular Liver Fibrosis With Advanced Age

In *Alb (+) bcl-x fl/fl* livers, apoptotic hepatocytes were found to be frequently engulfed by neighboring hepatocytes as well as nonparenchymal cells (Figure 3*B*). On the other hand, infiltration of inflammatory cells was rarely observed. Therefore, apoptotic cells seemed to be quietly removed from the tissue. Despite the lack of inflammation, *Alb (+) bcl-x fl/fl* mice developed age-related liver fibrosis. The fibrotic process was characterized by the deposit of collagen and elastic fibers surrounding hepatocytes in the perivenular region, and in a linear pattern in the sinusoidal region (Figure 4*A*). To quantitatively evaluate collagen deposits in the liver, we measured hydroxyproline content in the liver samples (Figure 4*B*). There was no difference in hepatic hydroxyproline content between *Alb (+) bcl-x fl/fl* and *Alb (−) bcl-x fl/fl* mice at 1 month after birth. However, at 3 months and later, the hepatic hydroxyproline content gradually increased in *Alb (+) bcl-x fl/fl* mice and was significantly higher than that in *Alb (−) bcl-x fl/fl* mice. It should be noted that *Alb (+) bcl-x fl/fl* mice developed modest liver fibrosis but not liver cirrhosis. Indeed, hepatic hydroxyproline content in these mice did not reach the levels of mice chronically injected with carbon tetrachloride, which is one of the established models of severe liver fibrosis (Figure 4*B*).

A Role of TGF-β in Apoptosis-Induced Liver Fibrosis

Liver fibrosis is a multifactorial process and involves various cytokines and growth factors. Among them, TGF-β plays a central role in activating hepatic stellate cells, which in turn produce collagen fibers.[15] Several lines of transgenic mice showed that enforced expression of TGF-β generates liver fibrotic responses.[16,17] In the present study, enzyme-linked immunosorbent assay was used to determine the expression of TGF-β in *Alb (+) bcl-x fl/fl* livers. The levels of TGF-β1 content were significantly higher in *Alb (+) bcl-x fl/fl* livers than in *Alb (−) bcl-x fl/fl* livers as early as 1 month of age and also at later time points. However, they did not reach the levels seen in mice chronically injected with carbon tetrachloride (Figure 4*C*). Therefore, the increase in TGF-β production clearly precedes collagen fiber deposition in the *Alb (+) bcl-x fl/fl* liver tissues.

Although it was not possible to determine the cell types that produce TGF-β in the liver, we examined the hypothesis of whether professional as well as nonprofessional phagocytic cells in the liver produce TGF-β when engulfing

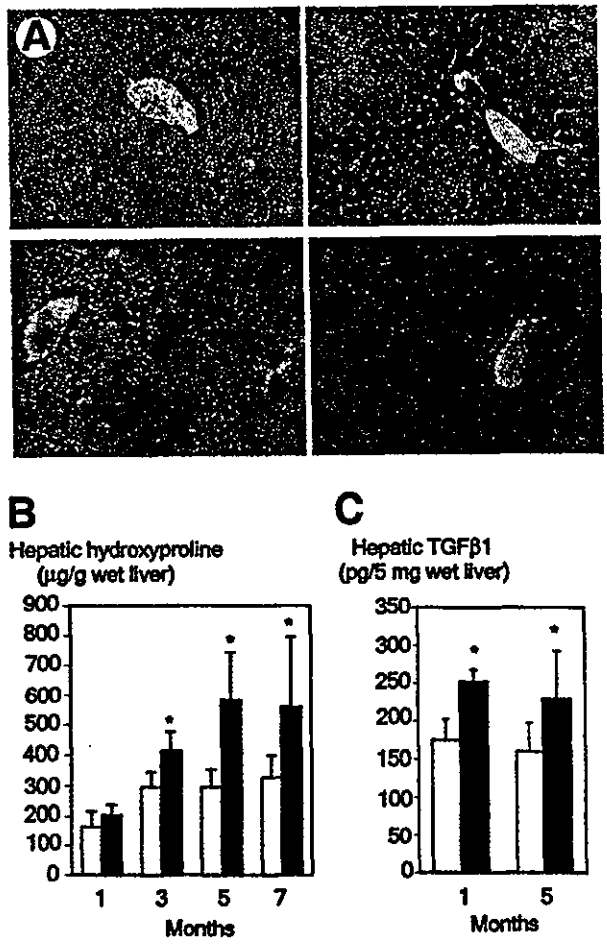

Figure 4. Fibrotic responses in hepatocyte-specific Bcl-x_L-deficient mice. (*A*) Masson's trichrome staining (*upper panels*) and silver staining (*lower panels*) of liver sections of 5-month-old *Alb* (+) *bcl-x fl/fl* (*left panels*) and *Alb* (−) *bcl-x fl/fl* mice (*right panels*). (*B*) Hepatic hydroxyproline content of *Alb* (+) *bcl-x fl/fl* (■) and *Alb* (−) *bcl-x fl/fl* (□) mice at various months after birth (n = 6/group). Mice chronically injected with carbon tetrachloride serving as a control had 950 ± 120 μg/g wet liver of hydroxyproline content. *$P < 0.05$ vs. *Alb* (−) mice. (*C*) TGF-β1 content in *Alb* (+) *bcl-x fl/fl* (■) and *Alb* (−) *bcl-x fl/fl* (□) *livers* at 1 and 5 months of age (n = 5/group). TGF-β1 content in the livers obtained from repeated carbon tetrachloride–injected mice was 480 ± 120 pg/5 mg wet liver. *$P < 0.05$ vs. *Alb* (−) *bcl-x fl/fl* mice.

apoptotic hepatocytes. Toward this goal, we cocultured murine macrophages (Raw264.7) or primary cultured hepatocytes with apoptotic hepatocytes that had been prepared by 2 days of infection with AdexCre of *bcl-x fl/fl* hepatocytes. Primary cultured hepatocytes as well as Raw264.7 macrophages were capable of engulfing apoptotic cells (Figure 5*A*), which is consistent with previous findings.[18] Notably, both cell types produced substantial levels of TGF-β1 into the culture supernatant in the presence of apoptotic hepatocytes (Figure 5*B*). The production of TGF-β1 required contact with apoptotic cells, because it was inhibited by the insertion of a Transwell membrane; this also excluded the possibility that residual adenoviruses that may exist in apoptotic cell cultures affect the production of TGF-β un-

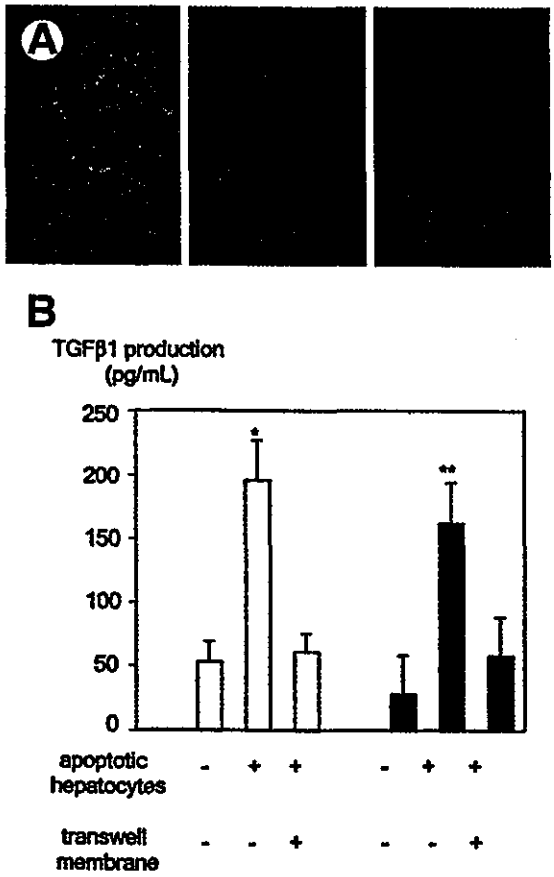

Figure 5. Production of TGF-β from professional and nonprofessional phagocytes in the presence of apoptotic cells. (*A*) Hepatocyte engulfment of apoptotic hepatocytes. 5(6)-carboxytetramethylrhodamine-labeled apoptotic hepatocytes were incubated with primary cultured hepatocytes. Apoptotic bodies were examined by fluorescence microscopy. Shown in the center is a representative photograph generated by merging phase contrast image (*left*) and red fluorescence image (*right*). Note apoptotic bodies within a cultured hepatocyte. (*B*) TGF-β production from murine macrophages RAW264.7 (*open bars*) and primary cultured hepatocytes (*closed bars*) in the presence or absence of apoptotic hepatocytes. In some experiments, Transwell membrane was inserted to separate apoptotic cells from hepatocytes or macrophages. $*P < 0.05$ vs. Raw264.7 single culture as well as Raw264.7 culture with apoptotic cells in a Transwell. $**P < 0.05$ vs. hepatocyte single culture as well as hepatocyte culture with apoptotic cells in a Transwell. Similar results were obtained in 3 independent experiments, and a representative result is shown.

der our experimental conditions. Taken together, these results suggest that residential macrophages as well as hepatocytes may produce TGF-β on exposure to apoptotic hepatocytes, which precedes liver fibrosis. However, we could not exclude the possibility that autocrine/paracrine production of TGF-β from hepatic stellate cells may contribute to at least a portion of the increase in TGF-β levels in our vivo in model.

Discussion

The present study clearly showed that hepatocytes cannot survive without expressing Bcl-x_L despite the presence of Bcl-w and Mcl-1, both of which have been shown to possess similar structures and share similar functions with Bcl-x_L.[19,20] The magnitude of apoptosis induced by Bcl-x_L disruption in vivo may appear less profound when compared with that seen in vitro. This may be partly related to the difficulty of detecting apoptosis in vivo due to the rapid phagocytosis and disappearance of apoptotic bodies followed by compensatory regeneration in the tissue. It is increasingly recognized that a variety of apoptotic stimuli converge on mitochondria via translocation of individual BH3-only proteins and that antiapoptotic members of the Bcl-2 family function as inhibitors of apoptosis on the mitochondrial outer membrane.[21] Our findings suggest that, even under physiologic conditions, hepatocytes always encounter various apoptotic insults that must be antagonized by Bcl-x_L to maintain cell integrity. Therefore, Bcl-x_L is a crucial apoptosis antagonist of hepatocytes.

Of interest is the finding that the spontaneous and continuous hepatocyte apoptosis seen on a Bcl-x_L knockdown induced fibrotic responses in the liver. Research has shown that repeated administration of agonistic Fas antibody generates a fibrotic response in vital organs such as the lung[22] and liver.[11] In addition, Fas-deficient mice were found to be resistant to the profibrotic effect of bleomycin and cholestasis in the lung and liver, respectively.[23,24] Although these reports imply a role of apoptosis in the pathway to fibrosis, the specificity of the apoptotic insults (i.e., Fas agonist, bleomycin, or cholestasis) applied in those studies has not been clearly established.[25] For example, apoptosis in liver endothelial cells is also generated by the administration of Fas antibody and contributes to sinusoidal hemorrhage as well as inflammatory cell infiltration.[26] Possible alterations in lymphocyte cytokine release in Fas-deficient animals may affect the fibrotic response.[27,28] The Bcl-x_L knockdown model described in the present study more directly proved a causal relationship between apoptosis of parenchymal cells and fibrogenesis.

Bcl-x_L–deficient mice showed increased production of TGF-β1 followed by collagen deposition in the liver. To the best of our knowledge, there has been no report suggesting that Bcl-x_L functions as a direct suppressor for TGF-β expression. Also, we did not observe any increases in TGF-β1 concentration in the culture supernatant of *bcl-x fl/fl* hepatocytes on AdexCre infection (unpublished data, May 2003). Therefore, it is less likely that down-modulation of Bcl-x_L directly up-regulates TGF-β1 production in hepatocytes. Rather, we showed that hepatocytes as well as macrophages can produce TGF-β1 in the presence of apoptotic hepatocytes. Fadok et al.[29] and Huynh et al.[30] previously reported that inflammatory reaction is actively suppressed, both in vitro and in vivo, through the production of TGF-β from macrophages at the time of engulfment of

apoptotic cells. The present study suggests an additional role for the TGF-β produced in promoting fibrosis, particularly when excessive apoptosis continues for a long time. Recently, Canbay et al.[31] clearly showed that apoptotic cells can directly activate a human hepatic stellate cell line and stimulate TGF-β production from these cells. Therefore, there may be various mechanisms by which apoptosis initiates profibrotic responses. Hepatocyte apoptosis precedes fibrosis in a variety of liver diseases such as chronic viral hepatitis, alcoholic liver injury,[2,32] and nonalcoholic steatohepatitis.[3] Further understanding of the mechanisms of apoptosis-induced fibrogenesis should offer therapeutic implications for controlling the development of liver fibrosis and preventing consequent organ failure.

References

1. Bar PR. Apoptosis—the cell's silent exit. Life Sci 1996;59:369–378.
2. Galle PR, Hofmann WJ, Walczak H, Schaller H, Otto G, Stremmel W, Krammer PH, Runkel L. Involvement of the CD95 (Apo-1/Fas) receptor and ligand in liver damage. J Exp Med 1995;182:1223–1230.
3. Feldstein AE, Canbay A, Angulo P, Taniai M, Burgart LJ, Lindor KD, Gores GJ. Hepatocyte apoptosis and Fas expression are prominent features of human nonalcoholic steatohepatitis. Gastroenterology 2003;125:437–443.
4. Uhal BD, Joshi I, Hughes WF, Ramos C, Pardo A, Selman M. Alveolar epithelial cell death adjacent to underlying myofibroblasts in advanced fibrotic human lung. Am J Physiol 1998;275:L1192–L1199.
5. Takehara T, Liu X, Fujimoto J, Friedman SL, Takahashi H. Expression and role of Bcl-xL in human hepatocellular carcinomas. Hepatology 2001;34:55–61.
6. Tzung SP, Fausto N, Hockenbery DM. Expression of Bcl-2 family during liver regeneration and identification of Bcl-x as a delayed early response gene. Am J Pathol 1997;150:1985–1995.
7. Kovalovich K, Li W, DeAngelis R, Greenbaum LE, Ciliberto G, Taub R. Interleukin-6 protects against Fas-mediated death by establishing a critical level of anti-apoptotic hepatic proteins FLIP, Bcl-2 and Bcl-xL. J Biol Chem 2001;276:26605–26613.
8. Motoyama N, Wang F, Roth KA, Sawa H, Nakayama K, Nakayama K, Negishi I, Senju S, Zhang Q, Fujii S, Loh DY. Massive cell death of immature hematopoietic cells and neurons in Bcl-x-deficient mice. Science 1995;267:1506–1510.
9. Rucker EB III, Dierisseau P, Wagner KU, Garrett L, Wynshaw-Boris A, Flaws JA, Hennighausen L. Bcl-x and Bax regulate mouse primordial germ cell survival and apoptosis during embryogenesis. Mol Endocrinol 2000;14:1038–1052.
10. Postic C, Shiota M, Niswender KD, Jetton TL, Chen Y, Moates JM, Shelton KD, Lindner J, Cherrington AD, Magnuson MA. Dual roles for glucokinase in glucose homeostasis as determined by liver and pancreatic beta cell-specific gene knock-outs using Cre recombinase. J Biol Chem 1999;274:305–315.
11. Song E, Lee SK, Wang J, Ince N, Ouyang N, Min J, Chen J, Shankar P, Lieberman J. RNA interference targeting Fas protects mice from fulminant hepatitis. Nat Med 2003;9:347–351.
12. Kanegae Y, Lee G, Sato Y, Tanaka M, Nakai M, Sakaki T, Sugano S, Saito I. Efficient gene activation in mammalian cells by using recombinant adenovirus expressing site-specific Cre recombinase. Nucleic Acids Res 1995;23:3816–3821.
13. Takehara T, Takahashi H. Suppression of Bcl-xL deamidation in human hepatocellular carcinomas. Cancer Res 2003;63:3054–3057.
14. Morsy MA, Alford EL, Bett A, Graham FL, Caskey CT. Efficient adenoviral-mediated ornithine transcarbamylase expression in deficient mouse and human hepatocytes. J Clin Invest 1993;92:1580–1586.
15. Friedman SL. Molecular regulation of hepatic fibrosis, an integrated cellular response to tissue injury. J Biol Chem 2000;275:2247–2250.
16. Sanderson N, Factor V, Nagy P, Kopp J, Kondaiah P, Wakefield L, Roberts AB, Sporn MB, Thorgeirsson SS. Hepatic expression of mature transforming growth factor β1 in transgenic mice results in multiple tissue lesions. Proc Natl Acad Sci U S A 1995;92:2572–2576.
17. Kanzler S, Lohse AW, Keil A, Henninger J, Dienes HP, Schirmacher P, Rose-John S, zum Buschenfelde KH, Blessing M. TGF-β1 in liver fibrosis: an inducible transgenic mouse model to study liver fibrogenesis. Am J Physiol 1999;276:G1059–G1068.
18. McVicker BL, Tuma DJ, Kubik JA, Hindemith AM, Baldwin CR, Casey CA. The effect of ethanol on asialoglycoprotein receptor-mediated phagocytosis of apoptotic cells by rat hepatocytes. Hepatology 2002;36:1478–1487.
19. Gibson L, Holmgreen SP, Huang DC, Bernard O, Copeland NG, Jenkins NA, Sutherland GR, Baker E, Adams JM, Cory S. bcl-w, a novel member of the bcl-2 family, promotes cell survival. Oncogene 1996;13:665–675.
20. Chao JR, Wang JM, Lee SF, Peng HW, Lin YH, Chou CH, Li JC, Huang HM, Chou CK, Kuo ML, Yen JJ, Yang-Yen HF. mcl-1 is an immediate-early gene activated by the granulocyte-macrophage colony-stimulating factor (GM-CSF) signaling pathway and is one component of the GM-CSF viability response. Mol Cell Biol 1998;18:4883–4898.
21. Cory S, Huang DC, Adams JM. The Bcl-2 family: roles in cell survival and oncogenesis. Oncogene 2003;22:8590–8607.
22. Hagimoto N, Kuwano K, Miyazaki H, Kunitake R, Fujita M, Kawasaki M, Kaneko Y, Hara N. Induction of apoptosis and pulmonary fibrosis in mice in response to ligation of Fas antigen. Am J Respir Cell Mol Biol 1997;17:272–278.
23. Kuwano K, Hagimoto N, Kawasaki M, Yatomi T, Nakamura N, Nagata S, Suda T, Kunitake R, Maeyama T, Miyazaki H, Hara N. Essential role of the Fas-Fas ligand pathway in the development of pulmonary fibrosis. J Clin Invest 1999;104:13–19.
24. Canbay A, Higuchi H, Bronk SF, Taniai M, Sebo TJ, Gores GJ. Fas enhances fibrogenesis in the bile duct ligated mouse: a link between apoptosis and fibrosis. Gastroenterology 2002;123:1323–1330.
25. Chapman HA. A Fas pathway to pulmonary fibrosis. J Clin Invest 1999;104:1–2.
26. Janin A, Deschaumes C, Daneshpouy M, Estaquier J, Micic-Polianski J, Rajagopalan-Levasseur P, Akarid K, Mounier N, Gluckman E, Socie G. Ameisen JC. CD95 engagement induces disseminated endothelial cell apoptosis in vivo: immunopathologic implications. Blood 2002;99:2940–2947.
27. Shi Z, Wakil AE, Rockey DC. Strain-specific differences in mouse hepatic wound healing are mediated by divergent T helper cytokine responses. Proc Natl Acad Sci U S A 1997;94:10663–10668.
28. Cohen PL, Eisenberg RA. Lpr and gld: single gene models of systemic autoimmunity and lymphoproliferative disease. Annu Rev Immunol 1991;9:243–69.
29. Fadok VA, Bratton DL, Konowal A, Freed PW, Westcott JW, Henson PM. Macrophages that have ingested apoptotic cells in vitro inhibit proinflammatory cytokine production through autocrine/paracrine mechanisms involving TGF-β, PGE2, and PAF. J Clin Invest 1998;101:890–898.

30. Huynh MLN, Fadok VA, Henson PM. Phosphatidylserine-dependent ingestion of apoptotic cells promotes TGF-β1 secretion and resolution of inflammation. J Clin Invest 2002;109:41–50.
31. Canbay A, Taimr P, Torok N, Higuchi H, Friedman S, Gores GJ. Apoptotic body engulfment by a human stellate cell line is profibrogenic. Lab Invest 2003;83:655–663.
32. Natori S, Rust C, Stadheim LM, Srinivasan A, Burgart LJ, Gores GJ. Hepatocyte apoptosis is a pathologic feature of human alcoholic hepatitis. J Hepatol 2001;34:248–253.

Received February 16, 2004. Accepted July 8, 2004.

Address requests for reprints to: Norio Hayashi, M.D., Department of Molecular Therapeutics, Osaka University Graduate School of Medicine, 2-2 Yamada-oka, Suita, Osaka 565-0871, Japan. e-mail: hayashin@molbx.med.osaka-u.ac.jp; fax: (81) 6-6879-3449.

Supported by a Grant-In-Aid for Scientific Research from the Ministry of Education, Culture, Sports, Science, and Technology, Japan.

The authors thank K. Kobayashi for excellent technical assistance.

Concanavalin A Injection Activates Intrahepatic Innate Immune Cells to Provoke an Antitumor Effect in Murine Liver

Takuya Miyagi,[1] Tetsuo Takehara,[1] Tomohide Tatsumi,[1] Takahiro Suzuki,[1] Masahisa Jinushi,[1] Yoshiyuki Kanazawa,[1] Naoki Hiramatsu,[1] Tatsuya Kanto,[1] Shingo Tsuji,[2] Masatsugu Hori,[2] and Norio Hayashi[1]

Concanavalin A (ConA), directly injected into mice, induces T cell–mediated liver injury. However, it remains unclear whether ConA injection can activate innate immune cells, including natural killer (NK) cells and natural killer T (NKT) cells, both of which exist abundantly in the liver. Here we report that ConA injection stimulated interferon (IFN)-γ production from liver NKT cells as early as 2 hours after injection and augmented YAC-1 cytotoxicity of liver NK cells. ConA-induced NK cell activation required other types of immune cells and critically depended on IFN-γ. Because a nonhepatotoxic low dose of ConA was capable of fully activating both NKT cells and NK cells, we next addressed the possibility of ConA injection displaying an antitumor effect in the liver without liver injury. A nonhepatotoxic low-dose ConA injection augmented the cytotoxicity of liver NK cells against Colon-26 colon cancer cells and suppressed hepatic metastasis of Colon-26 cells in a NK cell– and IFN-γ–dependent manner. In conclusion, a nonhepatotoxic low dose of ConA might serve as an immunomodulator that can preferentially activate the innate immune cells to induce an antitumor effect against metastatic liver tumor. (HEPATOLOGY 2004;40: 1190–1196.)

Concanavalin A (ConA) injection into mice leads to immunomediated liver injury.[1] ConA has a high affinity toward the hepatic sinus, which results in activation of immune cells in the liver.[1,2] Several immune cell types such as T cells or Kupffer cells have been shown to be involved in ConA-induced liver injury.[1,3] Recently, it has been reported that natural killer T (NKT) cells could critically contribute to this liver injury, because Jα281 knockout mice and CD1 knockout mice—both of which lack NKT cells—were resistant to this type of liver injury, and adaptive transfer of NKT cells from wild-type mice into these knockout mice could cancel this resistance.[4,5] In addition, several proinflammatory cytokines such as interferon (IFN)-γ, tumor necrosis factor alpha, interleukin (IL)-1, IL-2, IL-12, and IL-18 were shown to be markedly upregulated in liver tissue after ConA injection.[6–9] In particular, IFN-γ was reported to be critically involved in liver injury because its development was significantly reduced in mice deficient in IFN-γ or treated with IFN-γ–neutralizing monoclonal antibody (mAb).[9–11] However, it remains to be fully elucidated what changes occur in liver lymphocytes—particularly innate immune cells, including natural killer (NK) cells as well as NKT cells—after ConA injection.

The liver contains an abundant proportion of NK cells and NKT cells compared with other immune organs.[12] NK cells, which display nonspecific cytotoxicity against tumor cells,[13] can be activated for increased cytotoxicity following stimulation by a variety of cytokines, including IL-2, IL-12, IL-15, or IFN-α/β.[14,15] NKT cells, which are characterized by the expression of surface markers of NK cells together with a single invariant T cell receptor for antigen,[16] can be activated in a T cell receptor for antigen–dependent manner recognizing α-galactosylceramide (α-GalCer) bound on

Abbreviations: ConA, concanavalin A; NK, natural killer; NKT, natural killer T; IFN, interferon; IL, interleukin; mAb, monoclonal antibody; α-GalCer, α-galactosylceramide; PBS, phosphate-buffered saline; ALT, alanine aminotransferase; LMNC, liver mononuclear cell; Ig, immunoglobulin; E/T, effector to target; anti-AGM1, anti-asialo GM1 antibody.

From the Departments of [1]Molecular Therapeutics and [2]Internal Medicine and Therapeutics, Osaka University Graduate School of Medicine, Osaka, Japan.

Received April 19, 2004; accepted August 8, 2004.

Supported by a Grant-in-aid for Scientific Research and the 21st Century COE program from the Ministry of Education, Culture, Sports, Science, and Technology of Japan, and a Grant-in-aid for Research on Hepatitis and BSE from the Ministry of Health, Labour, and Welfare of Japan.

Address reprint requests to: Norio Hayashi, Department of Molecular Therapeutics, Osaka University Graduate School of Medicine, Yamadaoka 2 -2, Suita, Osaka 565-0871, Japan. E-mail: hayashin@moltx.med.osaka-u.ac.jp; fax: (81) 6-6879-3449.

Published online in Wiley InterScience (www.interscience.wiley.com).

DOI 10.1002/hep.20447

CD1d.[17] In addition, NKT cells can be activated in a T-cell receptor for antigen–independent fashion through the action of several cytokines such as IL-2, IL-12, IL-15, and IL-18.[18–20] It has been shown that NK cells and NKT cells can inhibit tumor formation in the murine liver and that these antitumor effects can be further enhanced by IL-2, IL-12, or α-GalCer administration,[20–25] suggesting that these innate immune cells in the liver play a central role in the first-line defense against intrahepatic metastatic tumor cells.

In this study, we demonstrate that liver NKT cells and NK cells were activated after ConA injection. Interestingly, both types of cells were fully activated even on injection of a nonhepatotoxic low dose of ConA. Furthermore, ConA could cause an NK cell–dependent antitumor effect in the liver *in vivo*. This report focuses on the changes in the innate immune cells, NK cells as well as NKT cells, in the liver induced by ConA injection, and suggests the importance of these innate immune cells in the defense against intrahepatic metastasis of tumor cells.

Materials and Methods

Cells and Animals. YAC-1, a mouse lymphoma cell line sensitive to NK cells, was purchased from American Type Culture Collection (ATCC, Rockville, MD). Colon-26, a mouse colon cancer cell line derived from BALB/c mice, was provided by Dr. Takashi Tsuruo (Institute of Molecular and Cellular Biosciences, University of Tokyo, Tokyo, Japan).[26] Female BALB/c mice and BALB/c *nu/nu* (nude) mice were obtained from Clea Japan, Inc. (Tokyo, Japan). BALB/c background IFN-$\gamma^{-/-}$ mice were provided by Dr. Yoichiro Iwakura (Institute of Medical Science, University of Tokyo, Tokyo, Japan).[10] These mice were maintained in a temperature-controlled, specific pathogen–free room at the Institute of Experimental Animal Science, Osaka University Medical School, and treated with humane care according to National Institutes of Health guidelines. Seven- to nine-week-old mice were used in this study.

Injection of ConA and Evaluation of Liver Injury. ConA, purchased from Sigma (St. Louis, MO), was dissolved in pyrogen-free phosphate-buffered saline (PBS) and intravenously injected to mice through the tail vein. Serum and liver from individual mice were obtained 15 hours after injection. Serum alanine aminotransferase (ALT) activities were measured with a standard UV method using a Hitachi type 7170 automatic analyzer (Tokyo, Japan). Removed livers were fixed in 10% formalin, embedded in paraffin, thin sectioned, and stained with hematoxylin-eosin.

Preparation of Liver Mononuclear Cells. Mice were anesthetized with pentobarbital sodium and their abdomens were opened. The inferior caval vein and the portal vein were cut to enable blood outflow. The liver was removed and passed through a stainless steel mesh. The liver cell suspension was collected and parenchymal cells were separated from liver mononuclear cells (LMNCs) by centrifugation at 50*g* for 5 minutes. LMNC populations were purified by centrifugation through a Percoll gradient as described previously.[21]

Flow Cytometric Analysis. LMNCs were suspended in PBS supplemented with 0.3% wt/vol bovine serum albumin and 0.1% wt/vol sodium azide. To avoid the nonspecific binding of Abs to the Fcγ receptor, the cells were preincubated with anti-CD16/32 mAb. Cells were then incubated with a saturating amount (1 μg/10^6 cells) of fluorescein isothiocyanate–conjugated anti-CD69 mAb or isotype-matched control immunoglobulin (Ig); peridinin chlorophyll protein–conjugated anti-CD3e mAb; and either phycoerythrin-conjugated anti–NK cell (DX5) mAb, anti-CD4 mAb, anti-CD8a mAb, or α-GalCer–loaded CD1d tetramers. For intracellular IFN-γ staining, the cells were stained with fluorescein isothiocyanate–conjugated anti–IFN-γ mAb or isotype-matched control Ig after staining of cell surface markers followed by fixation and permeabilization with a Cytofix-Cytoperm kit according to the manufacturer's instructions (BD Pharmingen, San Diego, CA). The stained cells were analyzed with a FACScan (Becton Dickinson, Mountain View, CA), and the data were processed using CELLQuest software (Becton Dickinson). CD69 expression and IFN-γ production of $CD4^+$ T cells, $CD8^+$ T cells, NK cells, or NKT cells were analyzed on electronically gated $CD3e^+$ $CD4^+$, $CD3e^+$ $CD8a^+$, $CD3e^-$ $DX5^+$ or CD1d-tetramer–reactive cells, respectively. All mAbs and control Ig were obtained from BD PharMingen; phycoerythrin-conjugated α-GalCer–loaded CD1d tetramers were provided by Dr. Richard S. Blumberg (Brigham and Women's Hospital, Boston, MA) and Dr. Mitchel Kronenberg (La Jolla Institute for Allergy and Immunology, San Diego, CA).[27]

Cytotoxicity Assay. The cytotoxicity of prepared LMNCs against YAC-1 cells or Colon-26 cells was measured by a standard ^{51}Cr release assay as previously described.[21] Target cells (1×10^6) were labeled for 60 minutes at 37°C with 100 μCi of $Na_2{}^{51}CrO_4$ in 500 μL of RPMI 1640 medium supplemented with 10% heat-inactivated fetal calf serum. Labeled targets (5×10^3 cells/well) were incubated for 4 hours at 37°C in 96-well plates containing medium (total volume of 100 μL) and LMNCs at various effector to target (E/T) ratios.

Separation of LMNCs via DX5 Marker. Prepared LMNCs were used to isolate DX5-positive and DX5-negative cells via magnetic cell sorting using MACS

(Miltenyi Biotec, Gladbach, Germany) according to the manufacturer's protocol. The purity of the fraction of both DX5-positive and DX5-negative cells was more than 90%. The fraction of DX5-positive cells consisted of mainly $CD3e^-/DX5^+$ NK cells (more than 90%).

Experimental Liver Metastasis of Colon-26 Cells. Mice were anesthetized, and the spleen was exposed to allow direct injection of 3×10^4 viable Colon-26 cells in 150 μL of PBS. The spleen was then returned, and the abdomen and skin were surgically sutured. Two days after the tumor injection, the mice were randomly assigned to the ConA treatment group or the control group. ConA (0.05 mg/200 μL) or 200 μL of PBS was intravenously administered to each group of mice, respectively. Two weeks after the tumor injection, the livers of ConA-treated or PBS-treated mice were removed, and the weight was measured to examine intrahepatic tumor growth. The removed livers were fixed in 10% formalin, embedded in paraffin, thin sectioned, and stained with hematoxylin-eosin. The numbers of tumor foci in the broadest sections including the portion of the liver hilus were counted under light microscopy to evaluate intrahepatic tumor formation.

In Vivo *Depletion of NK Cells.* To deplete NK cells *in vivo*, we used 50 μL of anti-asialo GM1 antibody (anti-AGM1) (Wako, Osaka, Japan), which we previously showed can selectively deplete NK cells.[21] Mice were intrasplenically injected with Colon-26 cells (3×10^4/mouse) and, on the next day, intraperitoneally administered either 50 μL of anti-AGM1 or the same amount of control normal rabbit Ig (DAKO, Copenhagen, Denmark). Two days after the tumor burden, 0.05 mg of ConA or 200 μL of PBS was injected to each group of anti-AGM1–administered mice and that of control Ig-administered mice. Two weeks after the splenic injection, the mice of each group were sacrificed to evaluate tumor growth as described above.

Statistical Analysis. The statistical significance of differences between the two groups was determined by applying the Mann-Whitney *U* test. We defined the statistical significance as a *P* value less than .05.

Results

Dose Dependence of ConA-Induced Liver Injury. ConA-induced liver injury has been reported to peak 8 to 24 hours after injection.[2,7] To examine the degree of liver injury, we assessed the serum ALT activities of BALB/c mice 15 hours after various doses of ConA injection. Serum ALT activities were considerably elevated in the mice injected with more than 0.2 mg of ConA (Fig. 1). The elevation of serum ALT activity was accompanied by histological hepatocyte damage (data not shown). When the injected dose of ConA was lower than 0.1 mg, neither elevation of serum ALT activity nor histological hepatocyte damage was observed (Fig. 1; data not shown). For further analysis, a dose of 0.05 mg was considered to be a nonhepatotoxic low dose, and a dose of 0.4 mg was considered to be a hepatotoxic dose.

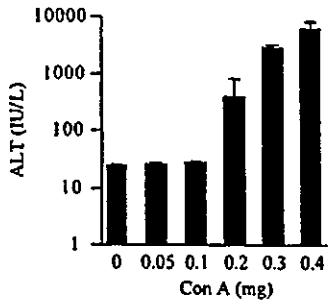

Fig. 1. Dose dependence of ConA-induced liver injury. BALB/c mice (n = 3) were injected intravenously with 200 μL of PBS containing the indicated doses of ConA. Serum ALT activity was determined 15 hours after the injection. Data are represented as the mean ± SE. ALT, alanine aminotransferase; Con A, concanavalin A.

Activation of Liver $CD4^+$ T and $CD8^+$ T Cells by ConA Injection. We investigated liver T cell activation after a nonhepatotoxic low dose as well as hepatotoxic dose of ConA injection. To this end, we evaluated the CD69 expression, an early activation marker,[28] and the IFN-γ production of liver $CD4^+$ T and $CD8^+$ T cells 15 hours after ConA injection. Although both doses of ConA upregulated CD69 expression and intracellular IFN-γ production of liver $CD4^+$ T cells and $CD8^+$ T cells, the upregulation induced by the nonhepatotoxic low dose (0.05 mg) was weaker, by about half, than that of the hepatotoxic dose (0.4 mg) (Fig. 2A, 2B).

Activation of Liver NKT Cells and NK Cells by ConA Injection. We investigated liver NKT cell activation after ConA injection of the nonhepatotoxic low dose as well as the hepatotoxic dose by comparison with that after the administration of 2 μg α-GalCer, provided by Kirin Brewery (Gumma, Japan), which has been shown to fully activate NKT cells in a CD1d-restricted manner.[21,29,30] Liver NKT cells began to decrease in number 2 hours after ConA- or α-GalCer injection and disappeared almost completely 12 hours after injection (data not shown). Therefore, CD69 expression and IFN-γ production of liver NKT cells were determined 2 hours after injection. Intracellular IFN-γ production of liver NKT cells was considerably upregulated by ConA injection of a nonhepatotoxic low dose as well as a hepatotoxic dose, both to the same degree as that by α-GalCer administration (Fig. 3A). Both doses of ConA injection upregulated CD69 expression at levels similar to that of α-GalCer administration (Fig. 3B).

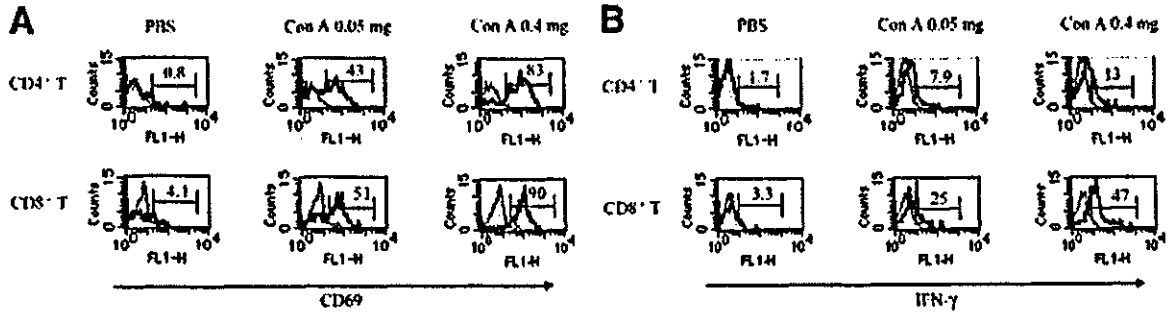

Fig. 2. Induction of CD69 expression and IFN-γ production of liver CD4+ T cells and CD8+ T cells by ConA injection. LMNCs were isolated from mice injected with 200 μL of PBS or the indicated doses of ConA 15 hours after injection. Cells were subjected to examination of CD69 expression and IFN-γ production of liver CD4+ T cells and CD8+ T cells. **Open and closed histograms** indicate staining with anti-CD69 mAb (A) or anti-IFN-γ mAb (B) and isotype-matched control Ig, respectively. Numbers indicate the percentage of (A) CD69+ cells or (B) intracellular IFN-γ+ cells. All experiments were done 3 times and representative data are shown. PBS, phosphate-buffered saline; Con A, concanavalin A; IFN-γ, interferon gamma.

Next, we investigated liver NK cell activation after ConA injection of the nonhepatotoxic low dose as well as the hepatotoxic dose. To this end, we evaluated the number, CD69 expression, and IFN-γ production of liver NK cells and the cytotoxicity of LMNCs against YAC-1 cells, which are sensitive to NK cell cytotoxicity, 15 hours after injection. The number of liver NK cells increased after ConA injection at doses of 0.05 mg and 0.4 mg, compared with that after PBS injection (0.99 ± 0.11, 1.19 ± 0.12, $0.41 \pm 0.04 \times 10^6$ cell/mouse, respectively). The CD69 expression and the intracellular IFN-γ production of liver NK cells were upregulated after ConA injection, and the upregulations caused by the 0.05-mg dose were nearly of the same degree as those caused by the 0.4-mg dose (Fig. 4A). The cytotoxicity against YAC-1 cells of LMNCs was remarkably augmented after ConA injection of both doses, and the augmentation caused by the 0.05-mg dose was nearly of the same degree as that of the 0.4-mg dose (Fig. 4B). Both doses of ConA injection augmented splenic mononuclear cell cytotoxicity, but to a much lesser extent (data not shown).

IFN-γ Dependence of Liver NK Cell Activation Induced by ConA Injection. Using nude mice, which have been shown to possess NK cells but not NKT cells or T cells (data not shown), we investigated whether NK cells were solely sufficient for their own activation after ConA injection. The cytotoxicity of LMNCs against YAC-1 cells in nude mice showed no augmentation after ConA injection at doses of 0.05 mg and 0.4 mg compared with that after PBS injection (Fig. 5A), suggesting the involvement of NKT cells and/or T cells in ConA-induced NK cell activation.

IFN-γ was produced considerably from liver NKT cells and to a lesser extent from liver T cells after ConA injection (Fig. 2B, 3A). We therefore investigated the contribution of IFN-γ to liver NK cell activation after ConA injection. ConA injection (at a dose of either 0.05 mg or 0.4 mg) had only a marginal effect on cytotoxicity against YAC-1 cells of LMNCs in IFN-$\gamma^{-/-}$ mice (Fig. 5B). In contrast, liver NKT cells in IFN-$\gamma^{-/-}$ mice upregulated CD69 expression and began to decrease in

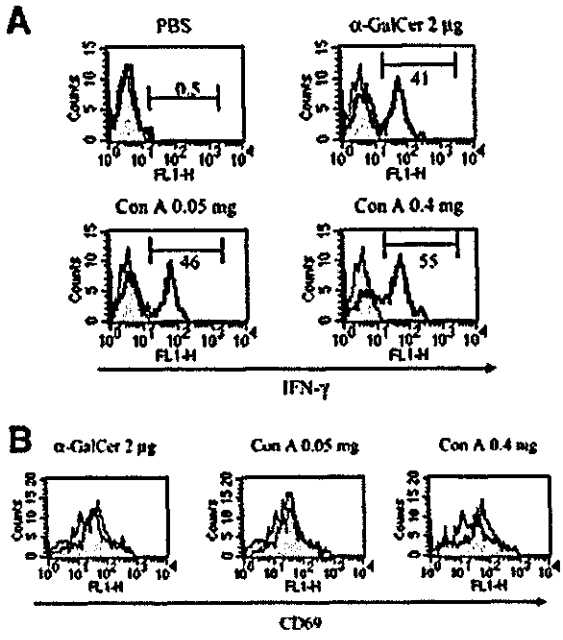

Fig. 3. Induction of intracellular IFN-γ production and CD69 expression of liver NKT cells by ConA injection. LMNCs were isolated from mice injected with 200 μL of PBS, 2 μg of α-GalCer, or the indicated doses of ConA 2 hours after injection. Cells were subjected to examination of (A) IFN-γ production and (B) CD69 expression of liver NKT cells. (A) **Open and closed histograms** indicate staining with anti-IFN-γ mAb and isotype-matched control Ig, respectively. Numbers indicate the percent of intracellular IFN-γ+ cells. (B) **Open and closed histograms** indicate the CD69 expression of PBS-injected mice and that of α-GalCer-injected or ConA-injected mice, respectively. Data are representative of 3 experiments. PBS, phosphate-buffered saline; α-GalCer, α-galactosylceramide; Con A, concanavalin A; IFN-γ, interferon gamma.

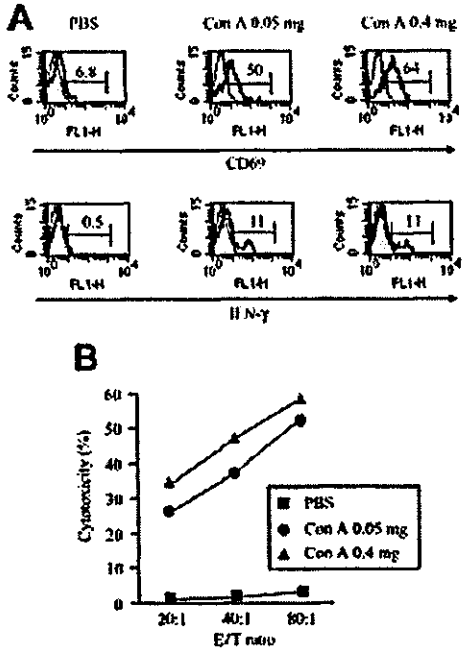

Fig. 4. Induction of CD69 expression and IFN-γ production of liver NK cells and cytotoxicity against YAC-1 cells of LMNCs by ConA injection. LMNCs were isolated from mice injected with 200 μL of PBS or the indicated doses of ConA 15 hours after injection. Cells were subjected to examination of CD69 expression and IFN-γ production of liver NK cells and examination of cytotoxicity of LMNCs against YAC-1 cells. (A) **Open and closed histograms** indicate staining with anti-CD69 mAb or anti-IFN-γ mAb and isotype-matched control Ig, respectively. Numbers indicate the percentage of $CD69^+$ cells or intracellular IFN-γ^+ cells. (B) Cytotoxicity of LMNCs against ^{51}Cr-labelled YAC-1 cells at the indicated E/T ratios. Data are representative of 3 experiments. PBS, phosphate-buffered saline; Con A, concanavalin A; IFN-γ, interferon gamma; E/T, effector to target.

number 2 hours after ConA injection at doses of both 0.05 mg and 0.4 mg (Fig. 5C) to the same degree as that after α-GalCer administration, observations that were identical to those in wild-type mice (Fig. 3B). These results demonstrate that either dose of ConA could activate liver NKT cells, but not liver NK cells, in IFN-$\gamma^{-/-}$ mice.

Antitumor Effect Against Metastatic Colon-26 Cells in the Liver by Nonhepatotoxic Low-Dose ConA Injection. Based on the findings that a nonhepatotoxic low-dose ConA injection could induce liver NK cell and NKT cell activation, we hypothesized that ConA injection might induce an antitumor effect in the liver without liver injury. We administered a nonhepatotoxic low dose of ConA into mice displaying 2-day intrahepatic metastasis of Colon-26 cells. Two weeks later, the number of tumor foci in the liver section of the mice in the ConA treatment group was significantly smaller than that in the control treatment group (Fig. 6A). Also, the liver weight of the mice in the ConA treatment group was significantly lighter than that in the control treatment group (Fig. 6B).

To examine whether NK cells were involved in this ConA-mediated antitumor effect, BALB/c mice were preinjected with anti-AGM1 to selectively deplete NK cells and were analyzed for the antitumor effect. There was no significant difference between the liver weights of the anti-AGM1–administered ConA treatment group and the anti-AGM1–administered PBS treatment group (n = 5; 3.8 ± 0.6 g, 3.0 ± 0.7 g, respectively). Because ConA-induced NK cell activation is critically dependent on IFN-γ (Fig. 5B), we also examined the antitumor effect in IFN-γ–deficient mice. There was no significant difference between the liver weights of the ConA-treated IFN-$\gamma^{-/-}$ mice group and the PBS-treated IFN-$\gamma^{-/-}$ mice group (n = 6; 3.4 ± 0.1 g, 4.0 ± 0.4 g, respectively).

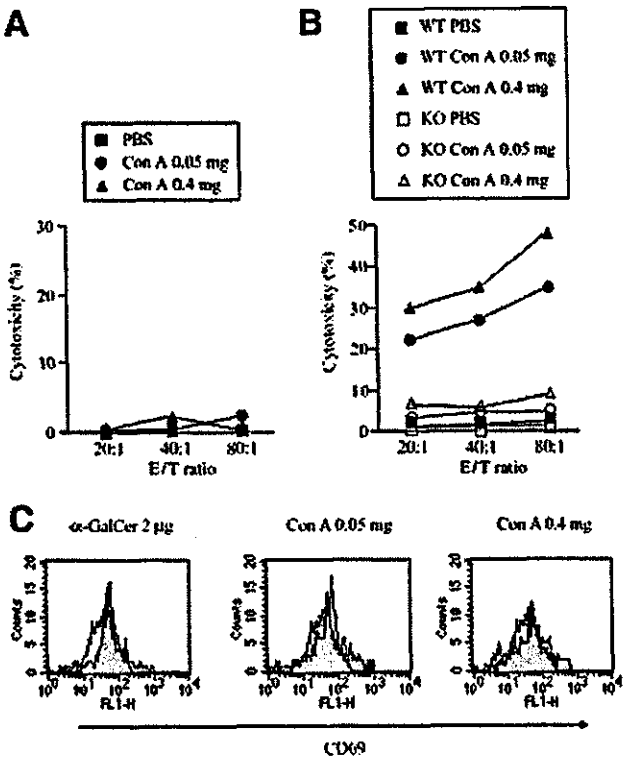

Fig. 5. Involvement of IFN-γ in liver NK cell activation by ConA injection. (A) Nude mice were injected with 200 μL of PBS or the indicated doses of ConA. Fifteen hours after the injection, LMNCs were isolated to examine the cytotoxicity against ^{51}Cr-labelled YAC-1 cells at the indicated E/T ratios. (B) IFN-$\gamma^{-/-}$ mice or wild-type mice were intravenously injected with 200 μL of PBS or the indicated doses of ConA. Fifteen hours after the injection, LMNCs were isolated from knockout or wild-type mice to examine the cytotoxicity against ^{51}Cr-labelled YAC-1 cells at the indicated E/T ratios. (C) LMNCs were isolated from IFN-$\gamma^{-/-}$ mice injected with 200 μL of PBS, 2 μg of α-GalCer, or the indicated doses of ConA 2 hours after injection. Cells were subjected to examination of CD69 expression of liver NKT cells. **Open and closed histograms** indicate the CD69 expression of PBS-injected mice and that of α-GalCer-injected or ConA-injected mice, respectively. Data are representative of 3 experiments. PBS, phosphate-buffered saline; Con A, concanavalin A; E/T, effector to target; WT, wild-type; KO, knockout; α-GalCer, α-galactosylceramide.

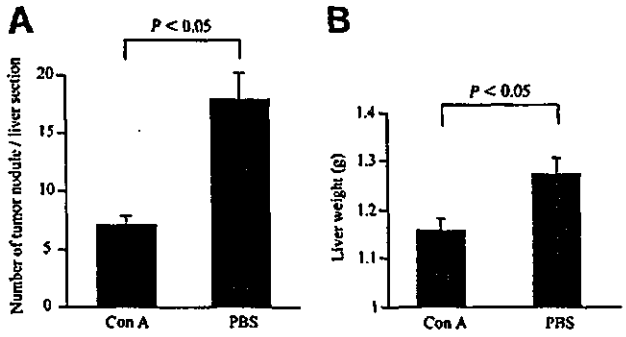

Fig. 6. Antitumor effect of nonhepatotoxic low-dose ConA injection *in vivo*. Tumor growth in the liver was estimated by (A) the number of tumor foci in the liver section and (B) the liver weight (n = 7). Data are represented as the mean ± SE and are representative of 3 experiments. Con A, concanavalin A; PBS, phosphate-buffered saline.

Augmentation of the Cytotoxicity of Liver NK Cells Against Colon-26 Cells by Nonhepatotoxic Low-Dose ConA Injection. Finally, we examined the cytotoxicity of liver NK cells against Colon-26 cells. The intrahepatic lymphocytes considerably augmented their cytotoxicity against Colon-26 cells after a nonhepatotoxic low-dose ConA injection compared with the control PBS injection (Fig. 7A). To characterize the lymphocyte subsets involved in this elevated cytotoxicity, the NK cell marker DX5-positive cells were separated from LMNCs and analyzed for their killing activity. DX5-positive cells killed Colon-26 cells much more efficiently than did preseparated LMNCs, while DX5-negative cells did not kill Colon-26 cells at all (Fig. 7B). These results agreed with the finding that NK cells were involved in the antitumor effect of a nonhepatotoxic low-dose ConA injection in the liver *in vivo*.

Discussion

In this study, we demonstrated that ConA injection into mice could induce the activation of innate immune cells, including NK cells and NKT cells, as well as T cells in the liver. Interestingly, liver NK cells and NKT cells could be fully activated by ConA injection even at a nonhepatotoxic low dose, while T cells were activated to a lesser degree than that observed after a hepatotoxic dose. This result is in line with mounting lines of evidence indicating that the activation of T cells plays an essential role in ConA-induced liver injury.

We have demonstrated here that liver NK cell activation after ConA injection could not be observed in nude mice in which NK cells are present but NKT cells and T cells are absent. This finding suggested that NK cells could not be directly activated by ConA injection and that NKT cells and/or T cells could be critically involved in NK cell activation after ConA injection. Although we did not directly address the question of which immune cell subset was involved in NK cell activation after ConA injection, we speculate that NKT cells are important for the following reasons. First, among the immune cell subsets tested, NKT cells were the earliest activated after ConA injection. Secondly, NKT cells produced the highest level of IFN-γ after ConA injection among the cell subsets tested. Importantly, NKT cells, but not NK cells, could also be activated after ConA injection in IFN-$\gamma^{-/-}$ mice. These findings suggested that IFN-γ produced from liver NKT cells might contribute to liver NK cell activation after ConA injection. However, further study is needed to clarify this point.

An important question is whether these activated NK cells were involved in ConA-induced liver injury. We observed that liver NK cell activation could be induced by ConA injection at a nonhepatotoxic low dose as well as a hepatotoxic dose to almost the same degree. Toyabe et al. reported that *in vivo* depletion of NK cells by anti-AGM1 administration did not inhibit ConA-induced liver injury,[31] which is consistent with our unpublished findings. Taken together with our findings and this report, we speculate that liver NK cell activation does not critically contribute to ConA-induced liver injury.

We have demonstrated that injection of a nonhepatotoxic low dose of ConA elicits an antitumor effect against metastatic Colon-26 colon cancer cells in the murine liver. This effect was critically dependent on the activation of NK cells, because the ConA injection could not suppress tumor growth in NK cell–depleted mice or IFN-γ–

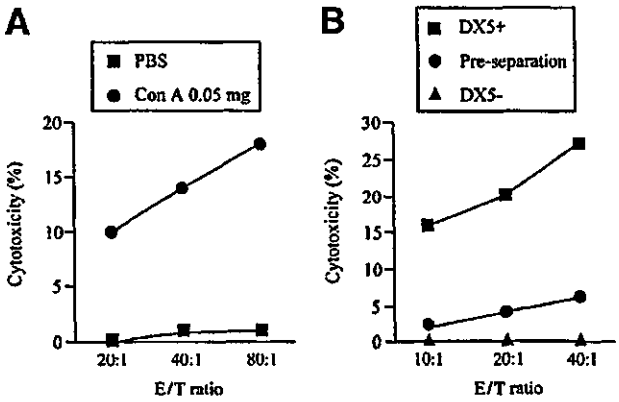

Fig. 7. Induction of cytotoxicity against Colon-26 colon cancer cells of liver NK cells by nonhepatotoxic low-dose ConA injection. Mice were injected with 200 μL of PBS or 0.05 mg of ConA. (A) Fifteen hours after the injection, LMNCs were isolated to examine the cytotoxicity against ^{51}Cr-labelled Colon-26 cells at the indicated E/T ratios. Also, prepared cells from 0.05 mg of ConA-injected mice (n = 15) were separated using NK cell marker DX5. (B) DX5-positive cells and DX5-negative cells as well as preseparated LMNCs were analyzed for cytotoxicity against ^{51}Cr-labelled Colon-26 cells at the indicated E/T ratios. Data are representative of 3 experiments. PBS, phosphate-buffered saline; Con A, concanavalin A; E/T, effector to target.